공학박사 학위논문

New Low-Complexity SLM Schemes and Clipping Noise Cancellation for OFDM Systems

OFDM 시스템을 위한 새로운 저 복잡도 SLM 방식 및 클리핑 잡음 제거 기법 연구

2015년 2월

서울대학교 대학원

전기컴퓨터공학부

김 기 훈

New Low-Complexity SLM Schemes and Clipping Noise Cancellation for OFDM Systems

지도 교수 노종선

이 논문을 공학박사 학위논문으로 제출함.

2014년 5월

서울대학교 대학원

전기컴퓨터공학부

김 기 훈

김기훈의 공학박사 학위논문을 인준함.

2014년 6월

위 원 장 _____ (인)

부위원장 _____ (인)

위 원 _____ (인)

위 원 _____ (인)

위 원 _____ (인)

New Low-Complexity SLM Schemes and Clipping Noise Cancellation for OFDM Systems

Presented to the Graduate School of Seoul National University in Partial Fulfillment of the Requirements for

THE DEGREE OF DOCTOR OF PHILOSOPHY

by

Kee-Hoon Kim

Department of Electrical Engineering and Computer Science

Seoul National University

This dissertation approved for

THE DEGREE OF DOCTOR OF PHILOSOPHY

June, 2014

Chairman _____

Vice Chairman _____

Member _____

Member _____

Member _____

Abstract

New Low-Complexity SLM Schemes and Clipping Noise Cancellation for OFDM Systems

Kee-Hoon Kim
Department of EE and CS
The Graduate School
Seoul National University

In this dissertation, several research results for the peak-to-average power ratio (PAPR) reduction schemes for orthogonal frequency division multiplexing (OFDM) systems are discussed. First, the basic principle and implementation of the OFDM systems are introduced, where high PAPR of OFDM signal is one of main drawbacks of OFDM systems. Thus, many PAPR reduction schemes to solve this problem have been studied such as clipping, selected mapping (SLM), partial transmit sequence (PTS), and tone reservation.

In the first part of this dissertation, a low-complexity SLM scheme is proposed, where the proposed SLM scheme generates alternative OFDM signal sequences by cyclically shifting the connections in each subblock at an intermediate stage of inverse fast Fourier transform (IFFT). Compared with the conventional SLM scheme, the proposed SLM scheme achieves similar PAPR reduction performance with much lower computational complexity and no bit error rate (BER) degradation. The performance of the proposed SLM scheme is analyzed mathematically and

verified through numerical analysis. Also, it is shown that the proposed SLM scheme has the lowest computational complexity among the existing low-complexity SLM schemes exploiting the signals at an intermediate stage of IFFT.

In the second part of this dissertation, an efficient selection (ES) method of the OFDM signal sequence with the minimum PAPR among many alternative OFDM signal sequences is proposed, which can be used for various SLM schemes. The proposed ES method efficiently generates each component of alternative OFDM signal by utilizing the structure of IFFT and calculates its power, and such generation procedure is interrupted if the calculated power is larger than the given threshold. By using the proposed ES method, the average computational complexity of considered SLM schemes is substantially reduced without degradation of PAPR reduction performance, which is confirmed by analytical and numerical results.

In the third part of this dissertation, a clipping noise cancellation scheme using compressed sensing (CS) technique is proposed for OFDM systems. The proposed scheme does not need reserved tones or pilot tones, which is different from the previous works using CS technique. Instead, observations of the clipping noise in data tones are exploited, which leads to no loss of data rate. Also, in contrast with the previous works, the proposed scheme selectively exploits the reliable observations of the clipping noise instead of using whole observations, which results in minimizing the bad influence of channel noise. From the selected reliable observations,

the clipping noise in time domain is reconstructed and cancelled by using CS technique. Simulation results show that the proposed scheme performs well compared to other conventional clipping noise cancellation schemes and shows the best performance in the severely clipped cases.

Keywords: Clipping, compressed sensing (CS), orthogonal frequency division multiplexing (OFDM), peak-to-average power ratio (PAPR), selected mapping (SLM).

Student ID: 2010-30210

Contents

List of Tables

List of Figures

Chapter 1. Introduction

1.1. Background

Orthogonal frequency division multiplexing (OFDM) is a multicarrier modulation method utilizing the orthogonality of subcarriers. OFDM has been adopted as a standard modulation method in several wireless communication systems such as digital audio broadcasting (DAB), digital video broadcasting (DVB), IEEE 802.11 wireless local area network (WLAN), and IEEE 802.16 wireless metropolitan area network (WMAN) [1].

OFDM is based on the frequency-division multiplexing (FDM), which is the method to transmit multiple data streams over a common spectrum. Each data stream is modulated onto multiple carriers within the bandwidth of the spectrum. In other words, the serial data stream is split into multiple low-rate data streams, and each is modulated onto a different subcarrier, where the subcarriers are orthogonal to each other. Then, all the modulated subcarriers are linearly superposed and transmitted. Weinstein devised the parallel data transmission system by using inverse discrete Fourier transform (IDFT), and then, it can be effectively implemented by inverse fast Fourier transform (IFFT) in 1971 [2]. Guard time also known as guard interval was proposed by cyclically extending the OFDM signal in 1980 [3]. This can remove inter-symbol interference (ISI)

and transform the linear convolution of OFDM signal and channel impulse response to cyclic convolution.

The parallel transmission of OFDM increases the symbol duration and it makes frequency selective fading channel to several flat fading channels. Therefore, OFDM has the immunity from frequency selective fading channel. Thus, in the OFDM system, the complex equalizer is not required because the one-tap equalizer sufficiently compensates the signal distortion by fading channel. Also, OFDM has an advantage of the spectral efficiency due to subcarrier orthogonality. OFDM subchannels whose spectra satisfy orthogonality can be overlapped each other, which can save the spectral efficiency up to 50% compared to FDM using unoverlapped spectrum. With excellent spectral efficiency, OFDM has become worthy in the wireless communication area.

Similar to other multicarrier schemes, OFDM has a high peak-to-average power ratio (PAPR) problem, which makes its straightforward implementation quite costly. High PAPR of OFDM signals leads to significant in-band distortion and out-of-band radiation when OFDM signals passes through nonlinear devices such as high power amplifier (HPA) [4]. Since linear range of HPA is limited, peak power of OFDM signals in time domain should be reduced. Thus, it is highly desirable to reduce the PAPR of OFDM signals [5]–[6].

Over the last decades, various techniques to reduce the PAPR of OFDM signals have been proposed such as clipping [7]–[9], coding [10]–[12], active constellation extension (ACE) [13], tone reservation (TR) [14], [15],

partial transmit sequence (PTS) [16], constellation shaping [17], and selected mapping (SLM) [18], [19]. Clipping is the simplest way to reduce the PAPR but it causes in-band distortion and bit error rate (BER) degradation. Coding has good PAPR reduction performance but it causes data rate loss. ACE extends the constellation on specific areas after a nonlinear process to reduce the PAPR, and it causes transmission power increase. TR reserves some subcarriers to reduce the PAPR, and it causes data rate loss. Constellation shaping is an approach to reduce the PAPR by increasing the constellation size of each subcarrier with keeping the average constellation power, but in many cases the minimum Euclidean distance is reduced and BER degradation occurs. SLM and PTS schemes are widely studied because they show good PAPR reduction performance without BER degradation. However, they require many IFFTs, which causes high computational complexity and needs to transmit the side information (SI) delivering which phase rotation vector was used. Also, SLM and PTS schemes require extra demodulation process at the receiver.

It is well known that the SLM scheme is more advantageous than the PTS scheme if the amount of SI is limited. However, the computational complexity of the SLM scheme is larger than that of the PTS scheme. Therefore, many modified SLM schemes with low-complexity have been proposed [20]-[27], but they have several shortcomings such as degradation of PAPR reduction performance or BER degradation compared to the conventional SLM scheme using the same number of alternative OFDM signal sequences. The low-complexity PAPR reduction algorithm in [22] causes

degradation of PAPR reduction performance because the used phase rotation vectors have periodicity, and thus they are highly correlated. The scheme in [23] shows BER degradation because it requires more pilot symbols and thus more power. The scheme in [24] shows somewhat degraded PAPR reduction performance because some phase rotation vectors are made by linear combination of other phase rotation vectors, which generates highly correlated phase rotation vectors.

1.2. Overview of Dissertation

The rest of this dissertation is organized as follows. In Chapter 2, OFDM system model is presented and PAPR of OFDM signals is defined. In Chapter 3, several PAPR reduction schemes for OFDM systems and their low-complexity algorithms are briefly explained.

In Chapter 4, a new low-complexity SLM scheme is proposed, which utilizes the signals at an intermediate stage of IFFT similar to [25] and [26]. However, the proposed scheme generates each alternative OFDM signal sequence by cyclically shifting the connections in each subblock at an intermediate stage of IFFT. It can also be equivalently viewed as multiplying the corresponding phase rotation vectors which have lower correlations than those of [25] and [26], to the input symbol sequence. Consequently, the PAPR reduction performance of the proposed SLM scheme can approach to that of the conventional SLM scheme with lower computational complexity compared to the schemes in [25] and [26]. Also, the proposed SLM scheme has no BER degradation compared to the conventional SLM

scheme.

In Chapter 5, an efficient selection (ES) method of the OFDM signal sequence with the minimum PAPR in the conventional SLM scheme is proposed, which can be applied to almost all of the existing SLM schemes including the low-complexity SLM schemes in [25], [22], [27]. By applying the proposed ES method, various SLM schemes are implemented with lower computational complexity, and the simulation results confirm that the ES method substantially reduces the average computational complexity of various SLM schemes. Note that the proposed ES method does not degrade the PAPR reduction performance of SLM schemes.

In Chapter 6, we propose a new clipping noise cancellation scheme using CS, which selectively uses observations of data tones. That is, reliable observations contaminated by less channel noise are selected, and then the clipping noise is reconstructed from these compressed observations by using a CS reconstruction algorithm. The proposed scheme does not reserve tones and instead exploits compressed observations of the underlying clipping noise in data tones, which leads to no data rate loss. The simulation results in Section 6.3 show that the proposed scheme mitigates the clipping noise well over both an additive white Gaussian noise (AWGN) channel and a Rayleigh fading channel.

Finally, some concluding remarks are given in Chapter 7, where the proposed techniques in the dissertation are reviewed.

Chapter 2. OFDM Systems

In a digital communication systems, a symbol duration should be much larger than the delay spread of a channel in order to remove the ISI of the transmission system. But, it limits the possible data rate for a single carrier modulation scheme. To overcome this limitation, multicarrier modulation scheme splits the high-rate data stream into N substream with low data rate and transmits these substream data on N adjacent subcarriers. Since the data symbols are allocated in parallel over the frequency domain, the total bandwidth to transmit these symbols is not changed. Instead, a symbol duration increases by a factor of N and thus, transmission with N times higher data rate for a given delay spread is possible.

As one of practical multicarrier modulation schemes, OFDM uses orthogonal waveforms to modulate the substreams. In OFDM, the spectra of subcarriers are overlapped in contrast to the conventional FDM because subcarriers are orthogonal to each other. Each subcarrier can be separated at the demodulator without interference if orthogonality of subcarriers is guaranteed. The spectral overlapping among subcarriers provides better spectral efficiency.

Although OFDM provides high-rate data transmission and spectral efficiency, a main drawback of OFDM is the high PAPR. High PAPR implies that HPA must have an inefficiently large linear range, which leads to

use of very expensive HPA. Therefore, PAPR of OFDM signals should be reduced.

This chapter is organized as follows. First, in Section 2.1, we describe the mathematical representation of OFDM system. Second, PAPR is defined in the OFDM system and some related facts are described in Section 2.2.

2.1. OFDM System Model

OFDM converts a high-rate data stream into many low-rate data streams by dividing wideband spectrum. That is, the high-rate data stream is split into N low-rate data streams, modulated using N subcarriers, and transmitted over the channel. Each low-rate data stream is loaded on the subcarrier and all the N subcarriers are summed for transmission. Let $\mathbf{X} = [X(0), X(1), ..., X(N-1)]^T$ be the input symbol sequence, where $[\cdot]^T$ denotes transpose. Without loss of generality, $X(k)$'s are assumed to be statistically independent and identically distributed (i.i.d.) random variables with zero mean. Then, the continuous-time baseband OFDM signal is represented as

$$x(t) = \frac{1}{\sqrt{N}} \sum_{k=0}^{N-1} X(k) \exp\left(\frac{j2\pi kt}{T}\right), \qquad 0 \le t \le T \tag{2.1}$$

where T is the OFDM signal duration.

Let $\Delta t_L = T/LN$ be a sampling interval, where L is an oversampling rate. Then the discrete-time OFDM signal component sampled at time

$n\Delta t_L$ can be expressed as

$$x_L(n) = x(n\Delta t_L), \qquad n = 0, 1, ..., LN - 1$$

and we denote $\mathbf{x}_L = [x_L(0), x_L(1), ..., x_L(N-1)]^T$.

For Nyquist sampling case $L = 1$, let $\mathbf{x}_1 = \mathbf{x} = [x(0), x(1), ..., x(N-1)]^T$ be the OFDM signal sequence corresponding to $\mathbf{X}$. The relation between the input symbol sequence $\mathbf{X}$ in frequency domain and the OFDM signal sequence $\mathbf{x}$ in time domain can be expressed by IFFT as

$$\mathbf{x} = \text{IFFT}_N(\mathbf{X})$$

where $\text{FFT}_N(\cdot)$ and $\text{IFFT}_N(\cdot)$ denote N-point fast Fourier transform (FFT) and N-point IFFT, respectively.

That is, an OFDM signal component $x(n)$ is expressed as

$$x(n) = \frac{1}{\sqrt{N}} \sum_{k=0}^{N-1} X(k) W^{-kn} \tag{2.2}$$

where $W = e^{-j\frac{2\pi}{N}}$ and $n \in \mathbb{Z}_N = \{0, 1, 2, \cdots, N-1\}$. Note that, an L-times oversampled OFDM signal sequence $\mathbf{x}_L$ can also be obtained by IFFT after padding $\mathbf{X}$ with $(L-1)N$ zeros.

2.2. Peak-to-Average Power Ratio

Since OFDM signals are generated by summing N sinusoidal waves, the peak power of OFDM signals can be very large compared to its average power. When it passes through nonlinear device such as HPA, high

peak power of OFDM signals leads to both in-band distortion and out-of-band radiation. The in-band distortion degrades BER and the out-of-band radiation interferes with the signals in the adjacent frequency bands. Therefore, it is desirable to reduce peak power of OFDM signals.

2.2.1. Definition of PAPR

The PAPR is the ratio of the maximum instantaneous power divided by the average power of the OFDM signal. That is, the PAPR of the oversampled OFDM signal sequence $\mathbf{x}_L$ is defined as

$$\mathrm{PAPR}(\mathbf{x}_L) = \frac{\max_{0 \le n \le LN-1} |x_L(n)|^2}{E\{|x_L(n)|^2\}}$$

where $E\{\cdot\}$ is the ensemble average operator.

2.2.2. Distribution of PAPR

For large N, $x(n)$ becomes a complex Gaussian random variable by central limit theorem. Thus the envelope of $x(n)$, $|x(n)|$, becomes a Rayleigh distributed random variable. Also, if the N input symbols are statistically independent, the output of IFFT, N OFDM signal components are also statistically independent. Therefore, the probability that the magnitude of all N OFDM samples are smaller than certain threshold γ_0 is given as

$$\Pr\left(\max_{0 \le n \le N-1} |x(n)| < \gamma_0\right) = \Pr(|x(n)| < \gamma_0)^N = (1 - e^{-\gamma_0^2})^N. \qquad (2.3)$$

From (2.3), the probability that at least one magnitude of the N OFDM signal components exceeds a certain magnitude threshold γ_0, that is,

$\Pr(\text{PAPR}(\mathbf{x}) > \gamma_0)$, can be approximated as

$$\Pr(\text{PAPR}(\mathbf{x}) > \gamma_0) = 1 - (1 - e^{-\gamma_0^2})^N. \tag{2.4}$$

If we consider the continuous time OFDM signals, the distribution in (2.4) becomes a different form. In [30], the empirical approximation of the PAPR distribution for continuous case was suggested as

$$\Pr(\text{PAPR} > \gamma_0) = 1 - (1 - e^{-\gamma_0^2})^{\alpha N} \tag{2.5}$$

where Nee proposed that (2.5) is the most agreeable with continuous time result when $\alpha = 2.8$. Also, by mathematical analysis, Ochiai derived the PAPR distribution of the continuous time OFDM signal $x(t)$ as [31]

$$\Pr(\text{PAPR} > \gamma_0) \approx 1 - \exp\left(- \sqrt{\frac{\pi}{3}} N \gamma_0 e^{-\gamma_0^2} \right). \tag{2.6}$$

Chapter 3. PAPR Reduction Schemes

It has been known that the PAPR problem is an important issue in OFDM systems. Thus, several PAPR reduction schemes have been proposed such as clipping, SLM, PTS, TR, and so on. Each scheme has its own characteristic and trade-off between the PAPR reduction and other performances such as BER, complexity, or data rate loss.

In this chapter, we review the conventional PAPR reduction schemes and their advantages and disadvantages in terms of PAPR reduction capability, computational complexity, BER degradation, data rate loss, and power increase, etc.

This chapter is organized as follows. First, in Section 3.1, we describe the mathematical procedure of clipping scheme. Second, SLM scheme is described in Section 3.2. In Sections 3.3 and 3.4, several low-complexity SLM schemes and TR scheme are introduced, respectively.

3.1. Clipping

3.1.1. Clipping at Transmitter

Clipping is performed on the oversampled OFDM signal sequence because it mitigates peak regrowth after digital-to-analog (D/A) conversion. It is known that four-times ($L = 4$) oversampling is sufficient for that pur-

pose [32]. The clipped signal $\bar{x}_L(n)$ is given as

$$\bar{x}_L(n) = \begin{cases} x_L(n), & |x_L(n)| \leq A \\ A \cdot e^{j\angle x_L(n)}, & |x_L(n)| > A \end{cases} \tag{3.1}$$

where A is the clipping threshold. Then the clipping ratio γ is defined as

$$\gamma = \frac{A}{E\{|x_L(n)|\}}. \tag{3.2}$$

Clearly, the clipping ratio γ can take a value larger than one.

The clipped signal $\bar{x}_L(n)$ can be considered as the sum of $x_L(n)$ and the clipping noise $c_L(n)$ as

$$\bar{x}_L(n) = x_L(n) + c_L(n), \qquad 0 \leq n \leq LN - 1. \tag{3.3}$$

Since the envelope of $x_L(n)$ is Rayleigh distributed when N is sufficiently large, it is easily shown that the average clipped output energy is [33]

$$E\{||\bar{x}_L||_2^2\} = (1 - e^{-\gamma^2})E\{||x_L||_2^2\} \tag{3.4}$$

where $||\cdot||_2$ denotes l_2-norm.

In order to remove the out-of-band radiation due to the clipping operation, the clipped signal $\bar{x}_L(n)$ in time domain is transformed to the one in frequency domain by taking LN-point FFT. (Filtering is not needed when $L = 1$, which is referred to as "clipping at the Nyquist sampling rate".) That is, we have $\bar{\mathbf{X}}_L = \mathrm{FFT}_{LN}(\bar{\mathbf{x}}_L)$. After filtering out the out-of-band

components of $\bar{\mathbf{X}}_L$, we have clipped input symbol sequence $\bar{X}(k)$ as

$$\bar{X}(k) = X(k) + C(k), \qquad 0 \le k \le N-1 \tag{3.5}$$

where $C(k)$ is the clipping noise in frequency domain, and we call $C(k)$ observations of the clipping noise.

Finally, $x(n) + c(n),\ n = 0, 1, ..., N-1$, is transmitted, where $\mathbf{x} = \text{IFFT}_N(\mathbf{X})$ is the OFDM signal sequence and $\mathbf{c} = \text{IFFT}_N(\mathbf{C})$ is the clipping noise which has to be recovered and cancelled at the receiver. Fig. 3.1 summarizes the clipping procedure.

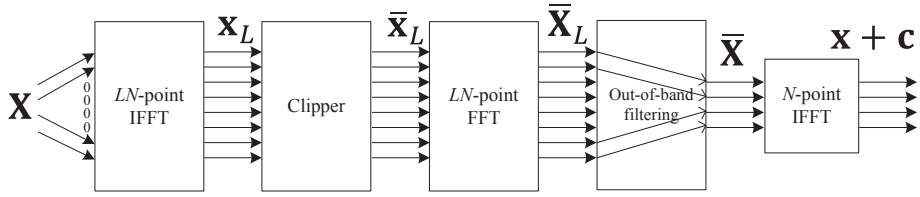

Figure 3.1: An example of clipping and filtering when $L = 2$ and $N = 4$.

3.1.2. A Statistical Model of Clipped Signals

Using the Bussgang's theorem, it was shown that the clipped signal $\bar{x}_L(n)$ can be statistically decomposed into two uncorrelated parts in [33] as

$$\bar{x}_L(n) = \alpha x_L(n) + d_L(n) \tag{3.6}$$

where α (≤ 1) is an attenuation factor and $d_L(n)$ is the oversampled clipping noise uncorrelated to $x_L(n)$. The attenuation factor α is given in

[33] as

$$\alpha = 1 - e^{-\gamma^2} + \frac{\sqrt{\pi}\gamma}{2}\mathrm{erfc}(\gamma).$$

Note that α is only dependent on γ, and thus α is known at the receiver when γ is fixed. From (3.6), the clipped input symbol sequence $\bar{X}(k)$ in (3.5) can be statistically viewed as

$$\bar{X}(k) = \alpha X(k) + D(k), \qquad 0 \le k \le N-1 \tag{3.7}$$

where $\mathbf{D}$ is the FFTed and out-of-band filtered version of $\mathbf{d}_L$, and clearly $\mathbf{C} = (\alpha - 1)\mathbf{X} + \mathbf{D}$.

$D(k)$ can be assumed to be a complex Gaussian random variable with zero mean and variance $2\sigma^2_{D(k)}$ [33]. For the Nyquist sampling rate ($L = 1$), its variance is easily obtained as

$$\begin{aligned} 2\sigma^2_{D(k)} &= E\{|\bar{X}(k)|^2\} - \alpha^2 E\{|X(k)|^2\} \\ &= (1 - e^{-\gamma^2} - \alpha^2) E\{|X(k)|^2\} \end{aligned} \tag{3.8}$$

and then

$$\begin{aligned} E\{|C(k)|^2\} &= (\alpha - 1)^2 E\{|X(k)|^2\} + 2\sigma^2_{D(k)} \\ &= (2 - 2\alpha - e^{-\gamma^2}) E\{|X(k)|^2\}. \end{aligned}$$

Even if $L > 1$, we can still obtain the values of $2\sigma^2_{D(k)}$ and $E\{|C(k)|^2\}$ for all k's. In many literatures [34]–[36], a power spectral density (PSD) of the oversampled clipping noise $\mathbf{d}_L$ is calculated from its autocorrelation

function in various forms. For example, the PSD of $\mathbf{d}_L$ is given as [34]

$$S_{\mathbf{d}_L\mathbf{d}_L}(v) = \sum_{n=1}^{\infty} \frac{\beta_n}{(E\{|X(k)|^2\})^{2n+1}} \cdot [\overbrace{S_{\mathbf{x}_L\mathbf{x}_L}(v) * \cdots * S_{\mathbf{x}_L\mathbf{x}_L}(v)}^{2n+1 \text{ convolutions}}] \quad (3.9)$$

where v is the frequency variable, β_n is a coefficient depending on the clipper, and $S_{\mathbf{x}_L\mathbf{x}_L}(v)$ is the PSD of a non-clipped signal. The exact expression of β_n can be found in [34]. Likewise, the values of $2\sigma^2_{D(k)}$ and $E\{|C(k)|^2\}$ can be calculated and stored in advance for any L. Note that, for all k's within $0 \leq k \leq N-1$, the values of $2\sigma^2_{D(k)}$ and $E\{|C(k)|^2\}$ when $L > 1$ are smaller than the values of those when $L = 1$, because when $L > 1$, the clipping noise spreads out over not only in-band but also out-of-band.

3.1.3. Conventional Receiver without Clipping Noise Cancellation Scheme

At the receiver, the received symbol $Y(k)$ in frequency domain can be expressed as

$$Y(k) = H(k)\bar{X}(k) + Z(k), \qquad 0 \leq k \leq N-1 \quad (3.10)$$

where $H(k)$ denotes the frequency domain channel response and $Z(k)$ denotes the AWGN with variance $2\sigma^2$. We assume the perfectly known channel response and the perfect synchronization which are widely adopted in many OFDM literatures such as [37] and [38]. After zero-forcing channel equalization, we obtain

$$H^{-1}(k)Y(k) = \bar{X}(k) + H^{-1}(k)Z(k). \quad (3.11)$$

Then, by plugging (3.7) into (3.11), we derive a maximum likelihood (ML) estimator for $X(k)$ as

$$\hat{X}(k) = \arg\min_{s\in\mathcal{X}} |\alpha^{-1}H^{-1}(k)Y(k) - s| \tag{3.12}$$

where $\mathcal{X}$ is a signal constellation.

3.2. Selected Mapping

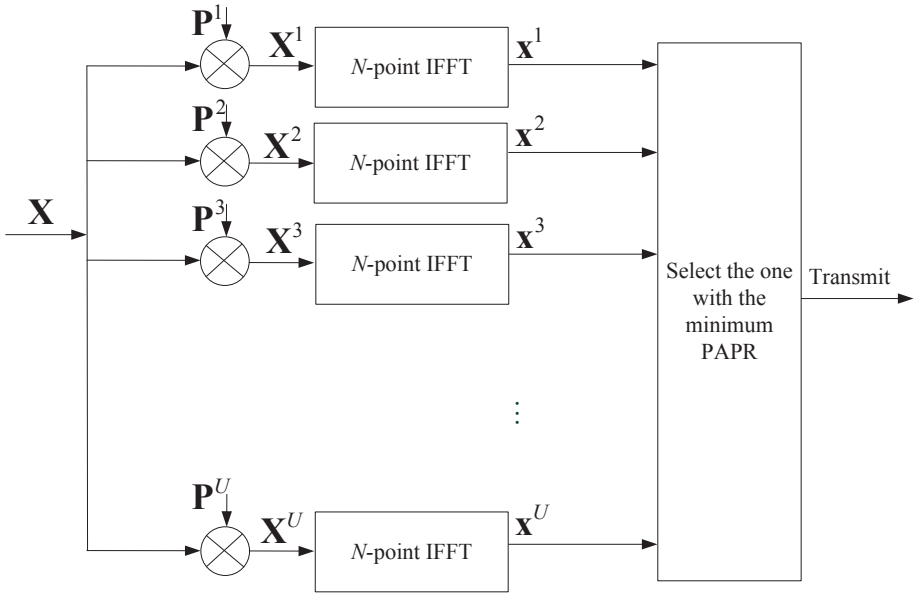

Figure 3.2: A block diagram of the conventional SLM scheme.

The conventional SLM scheme [18] is described in Fig. 3.2, which generates U alternative OFDM signal sequences $\mathbf{x}^u = [x^u(0), x^u(1), \cdots, x^u(N-1)]^T$, $1 \le u \le U$. To generate U alternative OFDM signal sequences, U distinct phase rotation vectors $\mathbf{P}^u$ known to both transmitter and receiver are used, where $\mathbf{P}^u$=$[P^u(0),\ P^u(1), \cdots,\ P^u(N-1)]^T$ with $P^u(k) = e^{j\phi^u(k)}$,

$\phi^u(k) \in [0,\ 2\pi)$, $1 \le u \le U$, and $\mathbf{P}^1$ is an all-one vector. Then, the input symbol sequence $\mathbf{X}$ is multiplied by each phase rotation vector $\mathbf{P}^u$ element by element to generate U distinct alternative input symbol sequences $\mathbf{X}^u = [X^u(0), X^u(1), \cdots, X^u(N-1)]^T$, where $X^u(k) = X(k)P^u(k)$.

Each of these U alternative input symbol sequences is IFFTed to generate total U alternative OFDM signal sequences $\mathbf{x}^u = \text{IFFT}_N(\mathbf{X}^u)$, and their PAPRs are calculated. Finally, the alternative OFDM signal sequence $\mathbf{x}^{\tilde{u}}$ having the minimum PAPR is selected for transmission as

$$\tilde{u} = \arg\min_{1 \le u \le U} \text{PAPR}(\mathbf{x}^u) = \arg\min_{1 \le u \le U} \left(\frac{\max_n |x^u(n)|^2}{E\{|x^u(n)|^2\}} \right)$$

where $E\{|x^u(n)|^2\} = E\{|x(n)|^2\}$ for all u's. Note that the SI on $\tilde{u}$ needs to be transmitted in order to properly demodulate the received OFDM signal sequence at the receiver, and U IFFTs are the dominant factors of the computational complexity in the conventional SLM scheme.

Pseudo code 1: the conventional SLM scheme

```
γ ⇐ ∞
for u = 1, 2, ··· , U
    Generate x^u by processing one N-point IFFT.
    if PAPR(x^u) < γ
        γ ⇐ PAPR(x^u)
        x^ũ ⇐ x^u
    end if
end for
Transmit x^ũ with the SI on ũ.
```

Pseudo code for the conventional SLM scheme is given as Pseudo code

1, where to find the OFDM signal sequence with the minimum PAPR, the value of γ is updated repetitively at each generation of alternative OFDM signal sequences. The value of γ in Pseudo code 1, called an *intermediate minimum PAPR value*, is the minimum among the PAPR values of the alternative OFDM signal sequences generated at that stage. For convenience, we use $\gamma^{(u)}$ to denote the value of γ after the PAPR of the u-th alternative OFDM signal sequence is compared, which is also represented as

$$\gamma^{(u)} = \min_{1 \le v \le u} \text{PAPR}(\mathbf{x}^v).$$

3.3. Low-Complexity SLM Schemes

In this section, three low-complexity SLM schemes are briefly reviewed, which have lower computational complexity than that of the conventional SLM scheme for the same number of alternative OFDM signal sequences.

3.3.1. Lim's SLM Scheme [25]

It is already known that one N-point IFFT consists of $l = \log_2 N$ stages. In Lim's SLM scheme, the N-point IFFT of the input symbol sequence $\mathbf{X}$ is processed from the first stage up to the $(l-r)$-th stage, not up to the l-th stage. Then, each of U phase rotation vectors, designed not to destroy the orthogonality between the subcarriers, is multiplied to the output from the $(l-r)$-th stage of the IFFT, and the remaining stages of IFFT, i.e., from the $(l-r+1)$-th stage to the l-th stage, are processed to generate total U alternative OFDM signal sequences. Among them, the

OFDM signal sequence with the minimum PAPR is transmitted.

3.3.2. Wang's SLM Scheme [22]

In Wang's SLM scheme, the input symbol sequence $\mathbf{X}$ is IFFTed to generate the original OFDM signal sequence $\mathbf{x}$. Then, $\mathbf{x}$ is multiplied by each of $U-1$ distinct $N \times N$ matrices, called conversion matrices, to generate alternative OFDM signal sequences. Then, among these U alternative OFDM signal sequences, the OFDM signal sequence with the minimum PAPR is transmitted.

3.3.3. Baxley's SLM Scheme [27]

The alternative OFDM signal sequences in Baxely's SLM scheme are generated by IFFT as the conventional SLM scheme, but the selection strategy is different. Suppose that the HPA used in the OFDM system is linear up to the saturation PAPR point γ_0. Then, achieving a PAPR value less than γ_0 does not help to improve the power efficiency of the HPA. Therefore, Baxely's SLM scheme stops generating more alternative OFDM signal sequences if an alternative OFDM signal sequence with PAPR less than γ_0 is found. With overwhelmingly low probability, all the U alternative OFDM signal sequences have PAPR values larger than γ_0 for the practical value of U, and in this case Baxely's SLM scheme clearly selects the one with the minimum PAPR.

3.4. Tone Reservation

The TR scheme reserves some tones for generating a PAPR reduction signal instead of data transmission [14]. Let $\mathcal{R} = \{i_1, i_2, \cdots, i_W\}$ denote the ordered index set of the reserved tones and $\mathcal{R}^{\mathrm{c}}$ denote the complement set of $\mathcal{R}$ in $\{0, 1, \cdots, N-1\}$, where W is the numbers of the reserved tones. Then, the input symbol $X(k)$ is expressed as

$$X(k) = A(k) + C(k) = \begin{cases} C(k), & k \in \mathcal{R} \\ A(k), & k \in \mathcal{R}^{\mathrm{c}} \end{cases}$$

where $A(k)$ is the data symbol with 0 in the peak reduction tone (PRT) set $\mathcal{R}$ and $C(k)$ is the PAPR reduction symbol with 0 in the set $\mathcal{R}^{\mathrm{c}}$, where they are not overlapped. Let $x(n)$, $a(n)$, and $c(n)$ be the time domain signals obtained by IFFTing $X(k)$, $A(k)$, and $C(k)$, respectively. Since IFFT is a linear operation, the OFDM signal $x(n)$ corresponds to the summation of the data signal $a(n)$ and the PAPR reduction signal $c(n)$, i.e., $x(n) = a(n) + c(n)$. Here, it is possible that well designed PAPR reduction signal $c(n)$ can reduce the PAPR of the original OFDM signal $a(n)$.

Next, we consider the generation method of peak reduction signals. It is very difficult to obtain the optimum values for PAPR reduction symbol $C(k)$. Thus, we introduce a well known method which is an iterative algorithm as follows. Let $\mathbf{f} = [f(0)\ f(1)\ \cdots\ f(N-1)]^T$ be the time domain

kernel signal defined by

$$f(n) = \frac{1}{\sqrt{N}} \sum_{k \in \mathcal{R}} F(k) e^{j2\pi \frac{k}{N} n}$$

where $F(k) = 0$ for $k \in \mathcal{R}^{\mathrm{c}}$. The kernel signal $\mathbf{f}$ can be computed in advanced and is used to make the PAPR reduction signal sequence $\mathbf{c}$ by an iterative manner. [14]. That is, the PAPR reduction signal sequence $\mathbf{c}^l$ at the lth iteration is obtained as

$$\mathbf{c}^l = \sum_{i=1}^{l} \alpha_i \mathbf{f}_{((\tau_i))}$$

where $\mathbf{f}_{((\tau_i))}$ denotes a circular shift of $\mathbf{f}$ by τ_i and α_i is a complex scaling factor computed according to the target threshold level γ_{th} and the maximum peak value at the ith iteration. The circular shift τ_i is determined as

$$\tau_i = \underset{0 \le n \le LN-1}{\arg\max} |a(n) + c(n)^{i-1}|.$$

Then, the OFDM signal sequence in the TR scheme at the lth iteration can be represented as

$$\mathbf{x} = \mathbf{a} + \mathbf{c}^l. \tag{3.13}$$

Chapter 4. A New Low-Complexity SLM Scheme for OFDM Systems

Several low-complexity SLM schemes which utilize the signals at an intermediate stage of IFFT have been proposed [25], [26]. In those schemes, the signals at an intermediate stage of IFFT are multiplied by phase rotation vectors to generate alternative OFDM signal sequences, which can be equivalently viewed as multiplying phase rotation vectors to the input symbol sequence. Although these schemes give PAPR reduction performance close to that of the conventional SLM scheme without BER degradation, their computational complexity is still high.

In this chapter, a low-complexity SLM scheme is proposed, which utilizes the signals at an intermediate stage of IFFT similar to [25] and [26]. However, the proposed scheme generates each alternative OFDM signal sequence by cyclically shifting the connections in each subblock at an intermediate stage of IFFT. It can also be equivalently viewed as multiplying the corresponding phase rotation vectors which have lower correlations than those of [25] and [26], to the input symbol sequence. Consequently, the PAPR reduction performance of the proposed SLM scheme can approach to that of the conventional SLM scheme with lower computational complexity compared to the schemes in [25] and [26]. Also, the proposed SLM scheme has no BER degradation compared to the conventional SLM

scheme.

The rest of this chapter is organized as follows. In Section 4.1, a new low-complexity SLM scheme is proposed and analyzed. The proposed SLM scheme is evaluated through simulation in Section 4.2 and conclusions are given in Section 4.3.

4.1. A New SLM Scheme with Low-Complexity

4.1.1. A New SLM Scheme

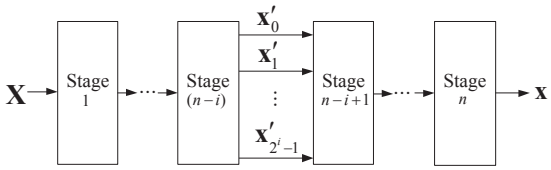

Figure 4.1: A block diagram of the ordinary N-point decimation-in-frequency IFFT ($n = \log_2 N$).

Prior to explaining the proposed SLM scheme, we describe the ordinary decimation-in-frequency radix-2 IFFT structure. It is well known that the ordinary N-point decimation-in-frequency IFFT can be viewed as in Fig. 4.1, where $n = \log_2 N$. For any integer i, $1 \leq i \leq n-1$, the intermediate OFDM signal sequence $\mathbf{x}'$ at stage $(n-i)$ is divided into 2^i subblocks $\mathbf{x}'_0, \mathbf{x}'_1, ..., \mathbf{x}'_{2^i-1}$. A subblock $\mathbf{x}'_m$ is composed of 2^{n-i} outputs from the stage $(n-i)$ of IFFT, which is equivalent to the 2^{n-i}-point IFFT using the input symbol sequence $X(k)$ satisfying $k \bmod 2^i = m$. Fig. 4.2 shows an example of subblock partitions when $N = 8$ and $i = 1,\ 2$.

Fig. 4.3 shows a block diagram of the proposed SLM scheme. The N

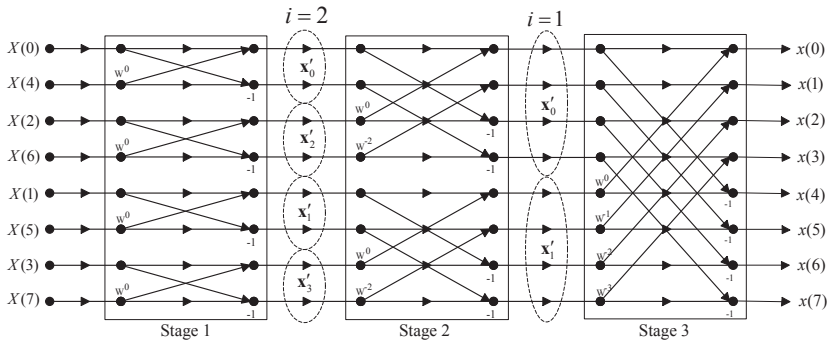

Figure 4.2: Subblock partitions at stage 1 (i.e., $i = 2$) and stage 2 (i.e., $i = 1$) of IFFT when $N = 8$ ($W = e^{-j\frac{2\pi}{8}}$).

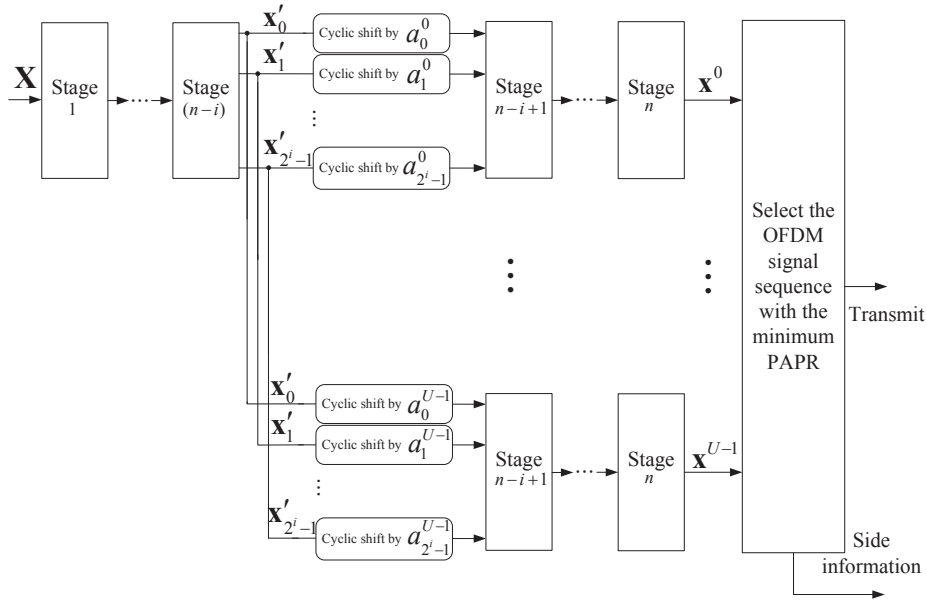

Figure 4.3: A block diagram of the proposed SLM scheme ($n = \log_2 N$).

input symbols $X(k)$, $0 \leq k \leq N-1$, are processed by the ordinary N-point decimation-in-frequency IFFT up to the stage $(n-i)$, where i is the number of remaining stages until finishing the IFFT. To generate the jth alternative OFDM signal sequence, $0 \leq j \leq U-1$, the connections in each of subblocks $\mathbf{x}'_0, \mathbf{x}'_1, ..., \mathbf{x}'_{2^i-1}$ are cyclically shifted upward by the predetermined integer numbers, $a_0^j, a_1^j, ..., a_{2^i-1}^j$, respectively. Note that performing the cyclic shift requires negligible computational cost. Then these cyclically shifted 2^i subblocks become the input to the stage $(n-i+1)$ of N-point IFFT to generate the jth alternative OFDM signal sequence $\mathbf{x}^j$. Finally, among these U alternative OFDM signal sequences, the one having the minimum PAPR is selected for transmission and the SI is also transmitted. In practical implementation of the proposed SLM scheme, the value of i and the values of $a_0^j, a_1^j, ..., a_{2^i-1}^j$ are fixed and thus the proposed SLM scheme needs $\lceil \log_2 U \rceil$ bits for SI, which is the same as the conventional SLM scheme's.

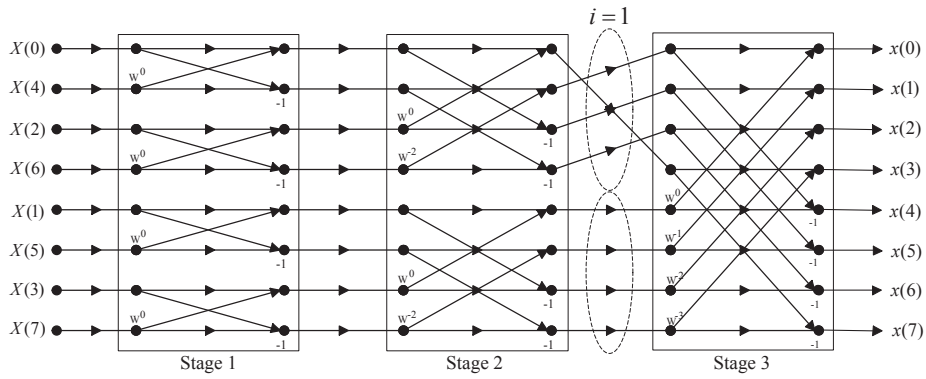

Figure 4.4: An alternative OFDM signal sequence generated by the proposed scheme for $N = 8$ and $i = 1$ using $a_0 = 1$ and $a_1 = 0$.

Fig. 4.4 shows an example to generate an alternative OFDM signal sequence by the proposed scheme for $N = 8$ and $i = 1$ using $a_0 = 1$ and $a_1 = 0$. Clearly, the original OFDM signal sequence $\mathbf{x}^0$ is generated by using $a_0 = 0$ and $a_1 = 0$. Other alternative OFDM signal sequences are generated by simply changing the shift values a_0 and a_1. For $i = 2$, each of four subblocks, $\mathbf{x}'_0, \mathbf{x}'_1, \mathbf{x}'_2, \mathbf{x}'_3$ is cyclically shifted and the last two stages of 8-point IFFT are performed as the ordinary IFFT.

The value i can be any of $1, 2, ..., n-1$. As i increases, the PAPR reduction performance improves but the computational complexity also increases, which will be explained in the following subsections. Also, a selection method of shift values $a_0^j, a_1^j, ..., a_{2^i-1}^j$ to achieve good PAPR reduction performance is analyzed and proposed in Sections 4.1.3 and 4.1.4. Compared with the conventional SLM scheme, the proposed scheme can substantially reduce the amount of computations for IFFTs to generate U alternative OFDM signal sequences, which will be analyzed in Section 4.1.5. Note that the proposed SLM scheme can also be implemented when radix-4 and split-radix IFFT algorithms are used. However, the radix-2 IFFT algorithm is usually used in practical systems and thus we describe the proposed SLM scheme with radix-2 IFFT structure.

4.1.2. Relation Between the Proposed SLM Scheme and the Conventional SLM Scheme

In this subsection, the relation between the proposed SLM scheme and the conventional SLM scheme is investigated. Let $M = 2^i$ be the number of subblocks at the stage $(n - i)$ in the N-point decimation-in-frequency

IFFT, where $N = 2^n$ and $L = N/M$ is the size of each subblock. Then, by replacing k with $Ml + m$ and ignoring the scaling factor $1/\sqrt{N}$ for convenience, (2.2) can be rewritten as

$$\begin{aligned} x(n) &= \sum_{m=0}^{M-1} \sum_{l=0}^{L-1} X(Ml+m) W^{-(Ml+m)n} \\ &= \sum_{m=0}^{M-1} \left(\sum_{l=0}^{L-1} X(Ml+m) W^{-Mln} \right) W^{-mn}. \end{aligned} \tag{4.1}$$

Note that $\sum_{l=0}^{L-1} X(Ml+m)W^{-Mln}, 0 \le m \le M-1$, in (4.1) corresponds to the subblock $\mathbf{x}'_m$ of the intermediate OFDM signal sequence at the stage $(n-i)$.

The jth alternative OFDM signal sequence is generated by cyclically shifting the connections in each subblock $\mathbf{x}'_m$ by a_m^j and processing the remaining stages of IFFT. Thus, the jth alternative OFDM signal sequence can be expressed as

$$\begin{aligned} x^j(n) &= \sum_{m=0}^{M-1} \left(\sum_{l=0}^{L-1} X(Ml+m) W^{-Ml(n+a_m^j)} \right) W^{-mn} \\ &= \sum_{m=0}^{M-1} \sum_{l=0}^{L-1} X(Ml+m) W^{-Mla_m^j} W^{-(Ml+m)n}. \end{aligned} \tag{4.2}$$

By replacing $Ml + m$ with k and noting that $m = k \bmod M$ and $Ml = k - (k \bmod M)$, the jth alternative OFDM signal sequence in (4.2) can be expressed as

$$x^j(n) = \sum_{k=0}^{N-1} X(k) W^{-(k-(k \bmod M))a^j_{k \bmod M}} W^{-kn}.$$

Clearly, the proposed SLM scheme can be equivalently viewed as the

conventional SLM scheme using the phase rotation vectors given as

$$P^j(k) = W^{-(k-(k \bmod M))a^j_{k \bmod M}}. \tag{4.3}$$

Therefore, the receiver of the proposed SLM scheme is identical to that of the conventional SLM scheme. Since the components of the phase rotation vectors used in the proposed SLM scheme are complex numbers with a unit magnitude (i.e., in (4.3), $|P^j(k)| = 1$ for all j and k), the proposed SLM scheme does not degrade the BER performance compared with the conventional SLM scheme.

4.1.3. Good Shift Values for the Proposed SLM Scheme

It is clear that the shift values have a big impact on the PAPR reduction performance of the proposed scheme. It is well known that the optimal phase rotation vectors should be orthogonal and aperiodic for SLM scheme [39]. However, for the correlated phase rotation vectors, the PAPR reduction performance can be analyzed by using the relation between the correlation of component powers of alternative OFDM signal sequences and the correlation of phase rotation vectors as in [40].

Let $\mathrm{P_c}^j(n)$, $0 \le n \le N-1$, denote the nth component power $|x^j(n)|^2$ of the jth alternative OFDM signal sequence $\mathbf{x}^j$. In [40], a design criterion of phase rotation vectors in SLM scheme with U alternative OFDM signal sequences was derived by using the correlation coefficient $\rho_{jv}(\tau)$ between $\mathrm{P_c}^j(n)$ and $\mathrm{P_c}^v(n+\tau)$, $0 \le \tau \le N-1$, where $0 \le j \ne v \le U-1$. It was also shown that the PAPR reduction performance improves as the maximum

value of $\rho_{jv}(\tau)$ for τ decreases. As in [40], $\rho_{jv}(\tau)$ can be approximated as

$$\rho_{jv}(\tau) \simeq \frac{1}{N^2}\left|\sum_{k=0}^{N-1} P^j(k)P^v(k)^* W^{k\tau}\right|^2 \tag{4.4}$$

where $(\cdot)^*$ denotes the complex conjugate. Therefore, to achieve good PAPR reduction performance, the shift values $\{a_0^j, a_1^j, ..., a_{M-1}^j\}$ and $\{a_0^v, a_1^v, ..., a_{M-1}^v\}$ should be chosen such that

$$\underset{a_0^j, a_1^j, ..., a_{M-1}^j, a_0^v, a_1^v, ..., a_{M-1}^v}{\arg\min} \left(\max_{\tau} \rho_{jv}(\tau)\right) \tag{4.5}$$

where $a_0^j, a_1^j, ..., a_{M-1}^j, a_0^v, a_1^v, ..., a_{M-1}^v \in \{0, 1, ..., L-1\}$. For solving this problem, by replacing k with $Ml + m$, we can rewrite (4.4) as

$$\rho_{jv}(\tau) \simeq \frac{1}{N^2}\left|\sum_{m=0}^{M-1}\sum_{l=0}^{L-1} P^j(Ml+m)P^v(Ml+m)^* W^{(Ml+m)\tau}\right|^2. \tag{4.6}$$

By using $P^j(Ml + m) = W^{-Mla_m^j}$ in (4.3), (4.6) can be given as

$$\begin{aligned}
\rho_{jv}(\tau) &\simeq \frac{1}{N^2}\left|\sum_{m=0}^{M-1}\sum_{l=0}^{L-1} W^{M(a_m^v - a_m^j + \tau)l + m\tau}\right|^2 \\
&= \frac{1}{N^2}\left|\sum_{m=0}^{M-1} \frac{W^{m\tau}((W^{M(a_m^v - a_m^j+\tau)})^L - 1)}{W^{M(a_m^v - a_m^j+\tau)} - 1}\right|^2 \\
&= \frac{1}{N^2}\left|A_0 + A_1 + ... + A_{M-1}\right|^2
\end{aligned} \tag{4.7}$$

where

$$A_m = \frac{W^{m\tau}((W^{M(a_m^v - a_m^j+\tau)})^L - 1)}{W^{M(a_m^v - a_m^j+\tau)} - 1},\ 0 \le m \le M-1. \tag{4.8}$$

Since $ML = N$, the term $(W^{M(a_m^v - a_m^j+\tau)})^L - 1$ in (4.8) is always zero because $(a_m^v - a_m^j + \tau)$ is an integer. Then, the numerator of A_m is always

zero and thus A_m is also zero except when the denominator of A_m is zero. When the denominator of A_m is zero, it is easy to show that $A_m = LW^{m\tau}$. The value of τ which generates nonzero A_m can be found by solving

$$a_m^v - a_m^j + \tau = 0 \bmod L.$$

Since $-L < a_m^v - a_m^j < L$ and $0 \le \tau < N$, the denominator of A_m becomes zero if

$$\tau = \begin{cases} c_0 L - (a_m^v - a_m^j), 1 \le c_0 \le M, & a_m^v - a_m^j \ge 0 \\ c_1 L - (a_m^v - a_m^j), 0 \le c_1 \le M-1, & a_m^v - a_m^j < 0. \end{cases} \tag{4.9}$$

For each m, as the integer τ runs from 0 to $N-1$, nonzero A_m appears M times. Therefore, it is clear that $\max_\tau \rho_{jv}(\tau)$ in (4.5) is minimized if A_m's are not overlapped each other. In other words, it is required that at most one A_m in (4.7) is nonzero for any τ, which can be achieved if the following condition is satisfied;

Condition for good shift values :

For all $m_1 \ne m_2$, $(a_{m_1}^v - a_{m_1}^j) - (a_{m_2}^v - a_{m_2}^j) \ne 0 \bmod L$.

If this condition is satisfied, the maximum value of $\rho_{jv}(\tau)$ becomes L^2/N^2. If this condition is not satisfied for some m, the maximum value of $\rho_{jv}(\tau)$ becomes larger than L^2/N^2. For instance, suppose that $a_{m_1}^v - a_{m_1}^j = a_{m_2}^v - a_{m_2}^j = d > 0$ for $m_1 \ne m_2$ and the condition is satisfied for other m's. Then, for $\tau = c_0 L - d$, $1 \le c_0 \le M$, we have $\rho_{jv}(\tau) \simeq$

$\frac{1}{N^2}|LW^{m_1\tau} + LW^{m_2\tau}|^2$ from (4.7) and it is easy to check that

$$\max_{1\le c_0\le M} \frac{1}{N^2} \mid LW^{m_1(c_0L-d)} + LW^{m_2(c_0L-d)} \mid^2 > \frac{L^2}{N^2}.$$

Similarly, if there are more than two distinct m's which do not satisfy the condition, it can be shown that the maximum value of $\rho_{jv}(\tau)$ is larger than L^2/N^2.

As a result, in order to achieve the best PAPR reduction performance of the proposed scheme with U alternative OFDM signal sequences, shift values should satisfy the condition for good shift values for all j, v pair, where $0 \le j \ne v \le U-1$. In this case, the maximum value of $\rho_{jv}(\tau)$ is L^2/N^2 for all j, v pair. Hence, for the same N, the PAPR reduction performance of the proposed scheme improves as i increases (i.e., L^2/N^2 decreases), which will be shown in Section 4.2.

4.1.4. Methods to Generate Good Shift Values

In this subsection, two methods to generate good shift values for the proposed SLM scheme are introduced. Firstly, random generation of shift values can be one of proper methods. If we choose a_m^j for all j and m from $\{0, 1, ..., L-1\}$ with equal probability $1/L$, then the term $(a_{m_1}^v - a_{m_1}^j) - (a_{m_2}^v - a_{m_2}^j)$ mod L can take the value from $\{0, 1, ..., L-1\}$ with equal probability. Therefore, shift values generated by the random generation method satisfy the condition for good shift values with high probability because the practical value of L is usually big. However, when we use the random generation method, both transmitter and receiver require the

memory space to save $M(U-1)$ shift values (except 0's for the original OFDM signal sequence).

Secondly, we introduce a deterministic method to generate the shift values satisfying the condition for good shift values. We set $a_m^j = mj$, which is called mj-method. Then, $(a_{m_1}^v - a_{m_1}^j) - (a_{m_2}^v - a_{m_2}^j)$ can be rewritten as

$$\begin{aligned}(a_{m_1}^v - a_{m_1}^j) - (a_{m_2}^v - a_{m_2}^j) &= (m_1 v - m_1 j) - (m_2 v - m_2 j) \\ &= (m_1 - m_2)(v - j). \end{aligned} \tag{4.10}$$

Since we only consider the case when $0 \le m_1 \ne m_2 \le M-1$ and $0 \le j \ne v \le U-1$, we obtain

$$0 < |(m_1 - m_2)(v - j)| \le (M-1)(U-1). \tag{4.11}$$

From (4.10) and (4.11), the mj-method is guaranteed to satisfy the condition for good shift values when $(M-1)(U-1) < L$, i.e., $(2^i - 1)(U-1) < 2^{n-i}$. This inequality can be satisfied for practical value of n and U because the appropriate value of i is 2 in the proposed scheme as will be shown in later section. Besides, the mj-method does not require the memory space to save the shift values, which is an additional advantage of the proposed SLM scheme using the mj-method compared to other SLM schemes requiring memory space to save the phase rotation vectors.

4.1.5. Computational Complexity

In this subsection, the computational complexity of the proposed scheme is compared with those of the conventional SLM scheme and other low-complexity SLM schemes. We only compare the computational complexity to generate alternative OFDM signal sequences because the remaining computational complexity is the same for most SLM schemes if the number of alternative OFDM signal sequences is the same.

When the number of subcarriers is $N = 2^n$, the numbers of complex multiplications and complex additions required for the conventional SLM scheme can be derived as follows. An N-point IFFT requires $(N/2)\log_2 N$ complex multiplications and $N\log_2 N$ complex additions. Therefore, the total numbers of complex multiplications and complex additions for the conventional SLM scheme using U alternative OFDM signal sequences are $U(N/2)\log_2 N$ and $UN\log_2 N$, respectively. In the proposed scheme, if the cyclic shifts are performed at the stage $(n-i)$, the numbers of required complex multiplications and complex additions are $((n-i)/n)(N/2)\log_2 N + U(i/n)(N/2)\log_2 N$ and $((n-i)/n)N\log_2 N + U(i/n)N\log_2 N$, respectively. Note that the reduction ratio of complex multiplications is the same as that of complex additions. Therefore, the computational complexity reduction ratio (CCRR) of the proposed scheme over the conventional SLM scheme is derived only for complex multiplication as

$$\begin{aligned}\text{CCRR} &= \left(1 - \frac{\text{Complexity of the proposed scheme}}{\text{Complexity of the conventional SLM}}\right) \times 100\ (\%) \\ &= \left(1 - \frac{n + (U-1)i}{nU}\right) \times 100\ (\%) = \frac{(n-i)(U-1)}{nU} \times 100\ (\%).\end{aligned}$$

Table 4.1: CCRR(%) of the Proposed Scheme Compared to the Conventional SLM.

N	64			256			1024		
U	4	8	16	4	8	16	4	8	16
$i = 1$	62.5	72.9	78.1	65.6	76.6	82.0	67.5	78.8	84.4
$i = 2$	50.0	58.3	62.5	56.3	65.6	70.3	60.0	70.0	75.0
$i = 3$	37.5	43.8	46.9	46.9	54.7	58.6	52.5	61.3	65.6
$i = 4$	25.0	29.2	31.3	37.5	43.8	46.9	45.0	52.5	56.3

As shown in Table 4.1, the proposed scheme has much lower computational complexity than the conventional SLM scheme. For example, when $i = 2, N = 1024$, and $U = 8$, the computational complexity of the proposed scheme reduces by 70% compared with the conventional SLM scheme with almost the same PAPR reduction performance. It is clear that the CCRR is large when N is large and i is small. However, for small i, there appears a large amount of degradation in the PAPR reduction performance compared to the conventional SLM scheme as will be shown in Section 4.2. Now, we compare the computational complexity of the existing low-complexity SLM schemes exploiting the signals at an intermediate stage of IFFT. The reason for this comparison is that their PAPR reduction performance is generally almost the same as that of the conventional SLM scheme with the same number of alternative OFDM signal sequences, which is different from most of other low-complexity SLM schemes.

Fig. 4.5 shows the comparison of the computational complexity of the proposed SLM scheme, the conventional SLM scheme, Lim's SLM

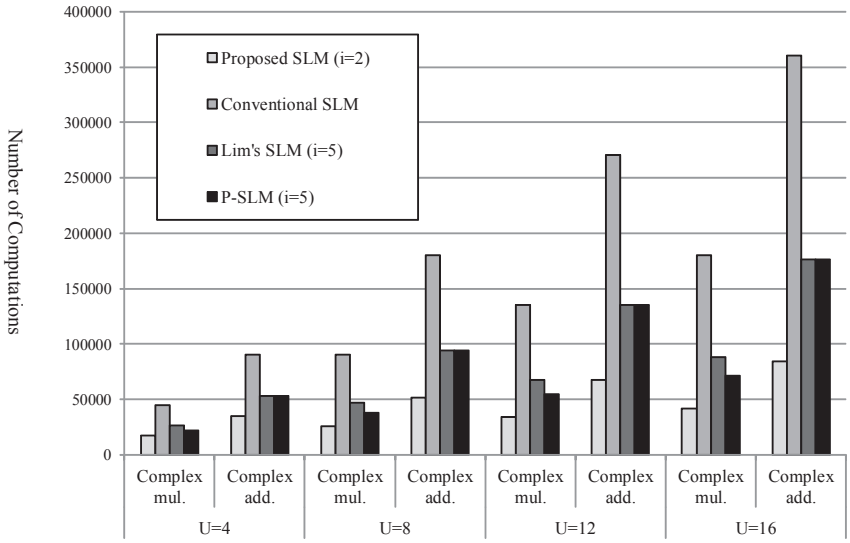

Figure 4.5: Comparison of the computational complexity of the proposed SLM, P-SLM [26], Lim's SLM [25], and the conventional SLM when $N = 2048$.

scheme [25], and P-SLM scheme [26]. We set each low-complexity scheme to have the PAPR reduction performance close to that of the conventional SLM scheme when $N = 2048$ and 16-quadrature amplitude modulation (16-QAM) is used. For the similar PAPR reduction performance compared to the conventional SLM scheme, the schemes in [25] and [26] need to exploit the signals at the 6-th intermediate stage of IFFT, which means $i = 5$. The proposed SLM scheme can give us the similar PAPR reduction performance compared to the conventional SLM scheme when $i = 2$ as will be shown in the Section 4.2. The computational benefit of the proposed SLM scheme mainly comes from this reason. As we expected, Fig. 4.5 shows that the proposed SLM scheme has the lowest computational complexity among these SLM schemes.

4.2. Simulation Results

For the simulation, 10^7 input symbol sequences are randomly generated and 16-QAM is used. The OFDM signal sequence is oversampled by a factor of four which is sufficient to represent the continuous OFDM signal. For the conventional SLM scheme, each element of the phase rotation vectors is randomly selected from $\{\pm 1, \pm j\}$. Similarly, to determine the shift values for the proposed SLM scheme, the random generation method is used. Note that the random generation method and the mj-method show almost the same PAPR reduction performance for the practical values of N, U, and i as will be shown in this section. However, in practical systems, the mj-method would be preferred because it does not require memory space to save the shift values. To evaluate the PAPR performance of the proposed SLM scheme, complementary cumulative distribution functions (CCDFs) are plotted.

Fig. 4.6 compares the PAPR reduction performance of the proposed SLM scheme with that of the conventional SLM scheme when $N = 1024$ and 16-QAM is used for $i = 1, 2, 3$. Fig. 4.6 shows that the PAPR reduction performance of the proposed SLM scheme becomes better as i increases, as expected from the analytical result that the maximum correlation coefficient value for the equivalent phase rotation vectors decreases as i increases. For example, the greatest gain of the computational complexity is obtained for $i = 1$, but the PAPR reduction performance is degraded due to the highly correlated equivalent phase rotation vectors.

It is also observed from Fig. 4.6 that the PAPR reduction performance of the proposed SLM scheme becomes closer to that of the conventional SLM scheme as i increases. When $i = 2$, both schemes show almost the same PAPR reduction performance. Since the performance of the proposed SLM scheme is lower bounded by that of the conventional SLM scheme and the computational complexity increases as i increases, the appropriate value of i can be 2.

Fig. 4.7 compares the PAPR reduction performance of the proposed SLM scheme using the mj-method and the random generation method for selecting shift values. Since they show almost the same PAPR reduction performance, we can expect that two methods show almost the same PAPR reduction performance for practical values of N, U, and i. However, the mj-method requires no memory space to save the shift values (i.e., $U-1$ phase rotation vectors), which is different from other SLM schemes.

4.3. Conclusions

In this chapter, a new low-complexity SLM scheme exploiting the signals at an intermediate stage of IFFT is proposed, which shows almost the same PAPR reduction performance as the conventional SLM scheme when $i = 2$. Instead of performing U IFFTs as in the conventional SLM scheme, the proposed scheme operates one IFFT up to $(n - i)$ stages, which is common to generation of all alternative OFDM signal sequences. Then, the connections in each subblock at the stage $(n - i)$ of IFFT is cyclically shifted by the predetermined shift value in the proposed SLM

scheme. Since the cyclic shifts at an intermediate stage of IFFT can be viewed as multiplying an equivalent phase rotation vector consisting of complex numbers with a unit magnitude to the input symbol sequence, there is no BER degradation compared to the conventional SLM scheme. Therefore, the proposed SLM scheme can be a good choice among many PAPR reduction schemes if the most important criterion of the PAPR reduction to consider is BER performance.

The simulation results show that the proposed SLM scheme using $i = 2$ can achieve almost the same PAPR reduction performance as the conventional SLM scheme. Also, it is verified that the proposed SLM scheme has the lowest computational complexity among existing low-complexity SLM schemes exploiting the signals at an intermediate stage of IFFT.

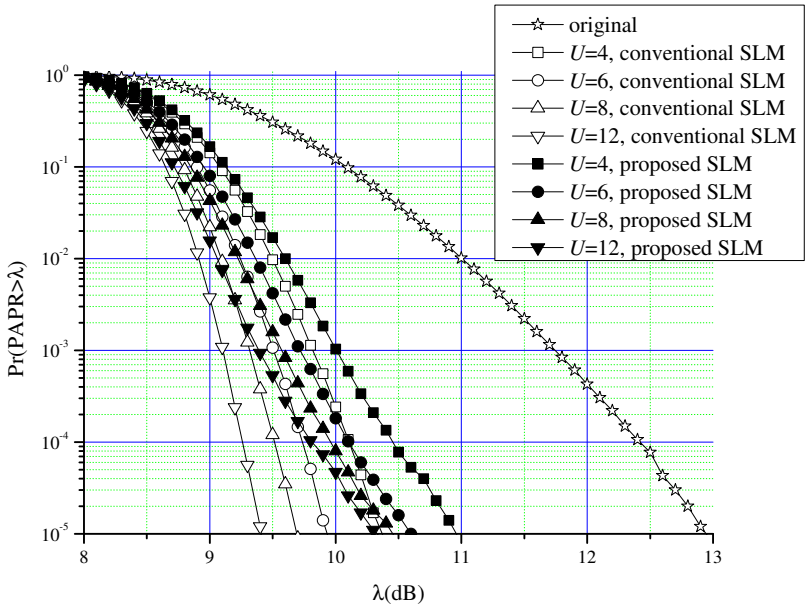
original
U=4, conventional SLM
U=6, conventional SLM
U=8, conventional SLM
U=12, conventional SLM
U=4, proposed SLM
U=6, proposed SLM
U=8, proposed SLM
U=12, proposed SLM
Pr(PAPR>λ)
λ(dB)

(a)

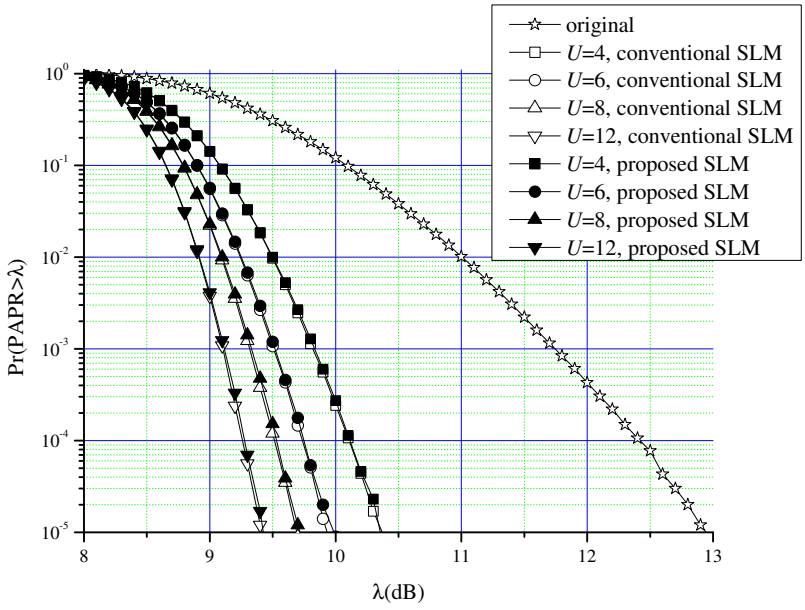
original
U=4, conventional SLM
U=6, conventional SLM
U=8, conventional SLM
U=12, conventional SLM
U=4, proposed SLM
U=6, proposed SLM
U=8, proposed SLM
U=12, proposed SLM
Pr(PAPR>λ)
λ(dB)

(b)

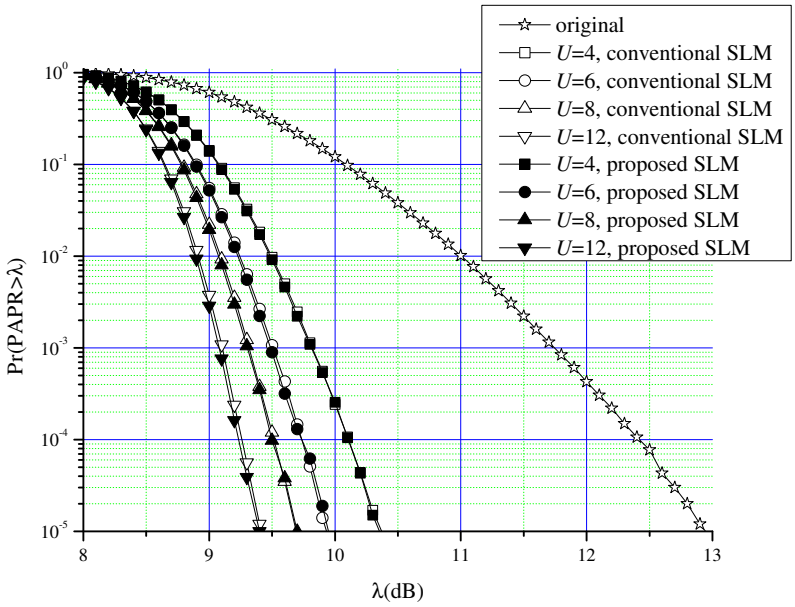

(c)

Figure 4.6: Comparison of PAPR reduction performance of the proposed and the conventional SLM schemes when $N = 1024$, and 16-QAM and four-times oversampling are used (a) $i = 1$, (b) $i = 2$, (c) $i = 3$.

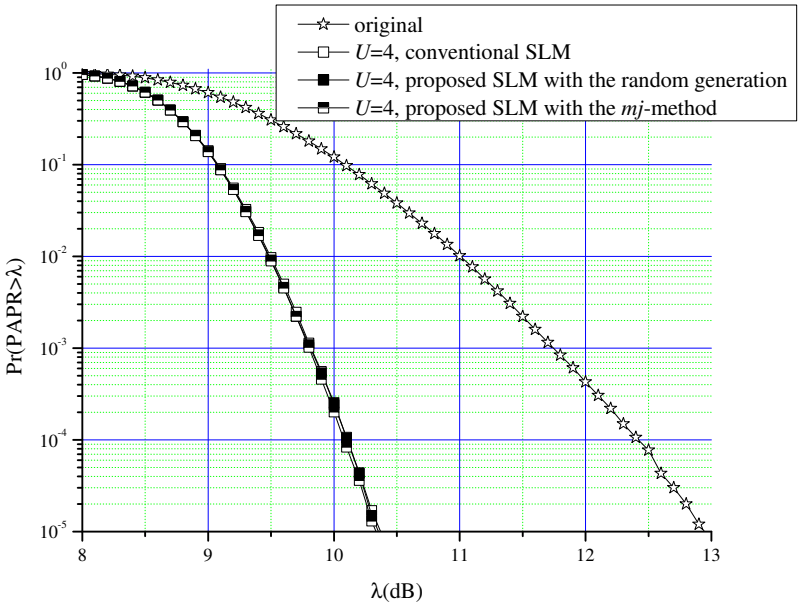

Figure 4.7: Comparison of the PAPR reduction performance of the proposed SLM scheme using the mj-method and the random generation method when $N = 1024$, $U = 4$, and $i = 3$, and 16-QAM and four-times oversampling are used.

Chapter 5. An Efficient Selection Method of a Transmitted OFDM Signal Sequence for Various SLM Schemes

In this chapter, an efficient selection (ES) method of the OFDM signal sequence with the minimum PAPR in the conventional SLM scheme is proposed, which can be applied to almost all of the existing SLM schemes including the low-complexity SLM schemes in [22], [25], [27]. By applying the proposed ES method, various SLM schemes are implemented with lower computational complexity and the simulation results confirm that the ES method substantially reduces the average computational complexity of various SLM schemes. Note that the proposed ES method does not degrade the PAPR reduction performance of SLM schemes.

The rest of the chapter is organized as follows. In Section 5.1, the ES method is introduced and applied to the conventional SLM scheme. Also, the computational benefit of the ES method is stochastically analyzed. In Section 5.2, the proposed ES method is applied to the three low-complexity SLM schemes. The computational benefit of the proposed ES method is evaluated through simulations in Section 5.3 and conclusions are given in Section 5.4.

5.1. ES Method and Its Application to the Conventional SLM Scheme

In this section, the ES method is proposed by explaining how to apply the ES method to the conventional SLM scheme.

5.1.1. Sequential Generation of OFDM Signal Components in the Conventional SLM Scheme

Alternative OFDM signal sequences are obtained by various generation methods such as IFFT in the conventional SLM scheme and multiplication of conversion matrices in Wang's SLM scheme. The proposed ES method utilizes the fact that such generation methods can be sequentially processed and in this subsection, we will explain how to sequentially generate OFDM signal components when alternative OFDM signal sequences are obtained by IFFT in the conventional SLM scheme.

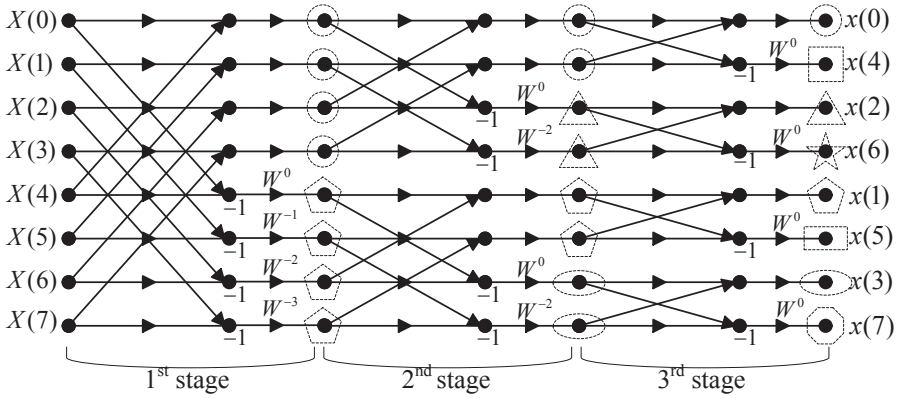

Figure 5.1: An 8-point IFFT structure in DIT and its nodes.

In the computational sense, it is widely known that an N-point IFFT requires total $N \log_2 N$ node values which are computed by complex addi-

tion and/or multiplication. The computational complexity of an IFFT is induced by these nodes and Fig. 5.1 shows an 8-point IFFT structure in decimation-in-time (DIT) with its 24 nodes. Generally, the OFDM signal components $x(0), x(4), x(2), \cdots, x(7)$ are generated by parallel computing the 24 nodes stage by stage.

On the other hand, a sequential generation of the OFDM signal components can be considered in IFFT. For example, the 24 nodes of the 8-point IFFT in Fig. 5.1 are marked by eight different dashed shapes. Clearly, $x(0)$ is generated by computing the seven 'dashed circle' nodes. Then $x(4)$ is generated by additionally computing only one 'dashed square' node, $x(2)$ is generated by computing three more 'dashed triangle' nodes, and then $x(6)$ is generated by computing one more 'dashed star' node.

$x(1)$ can be generated by computing the seven 'dashed pentagon' nodes. Clearly, $x(5)$, $x(3)$, and $x(7)$ are generated similarly to the case of $x(4)$, $x(2)$, and $x(6)$. Generally, in an N-point IFFT, the OFDM signal components $x(0), x(N/2), x(N/4), \cdots, x(N-1)$ in decimated order can be sequentially generated by doing a few more additional computation.

Sequential generation of the N-point IFFT values requires extra memory space for the $N \log_2 N$ nodes in addition to the N memory space required to implement the conventional IFFT. But, this storage requirement is not serious because the cost of the memory is cheap in these days.

5.1.2. Application of the ES Method to the Conventional SLM Scheme

At the u-th iteration in Pseudo code 1, after all the components of $\mathbf{x}^u$ are generated by performing N-point IFFT, the components' powers and PAPR($\mathbf{x}^u$) are computed and then the PAPR($\mathbf{x}^u$) is compared with $\gamma^{(u-1)}$. However, this is inefficient in terms of computational complexity.

It is easily shown that an efficient method can be obtained by utilizing the sequential generation in Section 5.1.1. While generating the u-th alternative OFDM signal sequence by the sequential generation, if a component power is larger than $\gamma^{(u-1)}E\{|x(n)|^2\}$, we stop the generation procedure immediately and move to the sequential generation of the $(u+1)$-th alternative OFDM signal sequence. Note that the PAPR reduction performance of the conventional SLM scheme is not affected by this interruption.

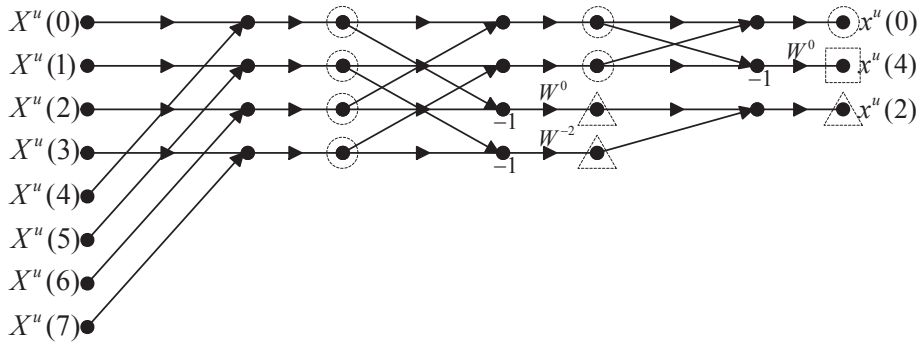

Figure 5.2: The eleven nodes required to generate the first three OFDM signal components $x^u(0)$, $x^u(4)$, and $x^u(2)$ in the u-th alternative OFDM signal sequence.

Clearly this interruption reduces the computational complexity due to

the u-th IFFT in the conventional SLM scheme. Suppose that the generation procedure of the u-th alternative OFDM signal sequence is interrupted after the first three OFDM signal components are generated when $N = 8$. Then, only the 11 nodes are computed in the u-th IFFT as shown in Fig. 5.2.

Pseudo code 2 shows a detailed procedure of the conventional SLM scheme aided by the proposed ES method. The third and fourth lines in Pseudo code 2 show the sequential generation of the components of the u-th alternative OFDM signal sequence. As the fifth, the sixth, and the seventh lines in Pseudo code 2 show, the sequential generation may be interrupted based on the value of γ and thus the average computational complexity of the conventional SLM scheme is possibly reduced. Fig. 5.3

Pseudo code 2: the conventional SLM scheme aided by the ES method

1: $\gamma \Leftarrow \infty$
2: **for** $u = 1, 2, \cdots, U$
3: **for** $n = 0, N/2, N/4, \cdots, N-1$ (in decimated order)
4: Generate $x^u(n)$ by the sequential generation in Section 5.1.1.
5: **if** $|x^u(n)|^2 > \gamma E\{|x(n)|^2\}$
6: go to 11.
7: **end if**
8: **end for**
9: $\gamma \Leftarrow \mathrm{PAPR}(\mathbf{x}^u)$
10: $\mathbf{x}^{\tilde{u}} \Leftarrow \mathbf{x}^u$
11: **end for**
12: Transmit $\mathbf{x}^{\tilde{u}}$ with the SI on $\tilde{u}$.

---

shows a block diagram of the conventional SLM scheme aided by the proposed ES method. Except the first IFFT block, at each IFFT block, the sequential generation of the components of each alternative OFDM signal sequence can be interrupted according to the value of $\gamma^{(u)}$.

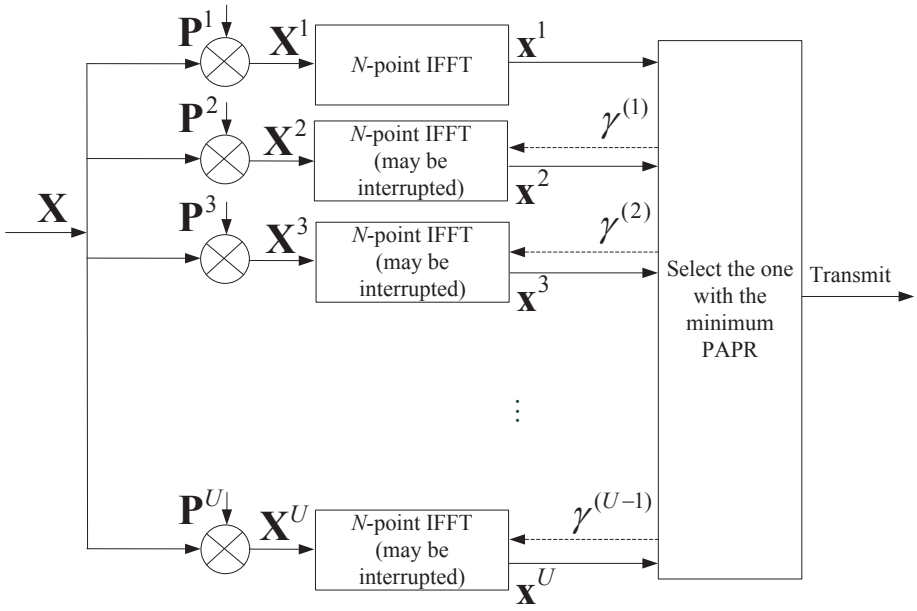

Figure 5.3: A block diagram of the conventional SLM scheme aided by the proposed ES method.

5.1.3. Complexity Analysis for Nyquist Sampling Case

In this subsection, we analyze the computational complexity of the conventional SLM scheme aided by the ES method for Nyquist sampling case. We only consider the computational complexity required to generate U alternative OFDM signal sequences by doing IFFTs, which is a dominant factor in the computational complexity of the SLM scheme. Also, we consider the computational complexity in an average sense because the

interruption of IFFT in the proposed ES method occurs depending on the random input symbol sequences.

Let B_u be the random variable of the number of generated OFDM signal components by the sequential generation at the u-th IFFT until an interruption occurs, $2 \leq u \leq U$. Let D_N denote the amount of computations for one N-point IFFT. Then we can obtain the average computational complexity of the conventional SLM scheme aided by the ES method as

$$D_N + \sum_{b_2=1}^{N} K_N(b_2) p_{B_2}(b_2) + \cdots + \sum_{b_U=1}^{N} K_N(b_U) p_{B_U}(b_U) \tag{5.1}$$

where $K_N(b)$ denotes the computational complexity to generate b OFDM signal components in an N-point IFFT by the sequential generation and $p_{B_u}(b_u)$ denotes the probability mass function (PMF) of B_u. Clearly, the computational complexity of the conventional SLM scheme with U alternative OFDM signal sequences without the ES method is UD_N.

5.1.3.1. Characteristics of a Nyquist-Sampled OFDM Signal Sequence

Prior to deriving the functions $K_N(b)$ and $p_{B_u}(b_u)$ in (5.1), we overview the characteristics of a Nyquist-sampled OFDM signal sequence $\mathbf{x}$.

As in many other works, it is assumed that an OFDM signal component is a complex Gaussian random variable with zero mean and $E\{|x(n)|^2\}$ variance, which is a good approximation for a large number of subcarriers from the central limit theorem [31]. Since an OFDM signal component is complex Gaussian, the amplitude of an OFDM signal component is Rayleigh distributed. Thus, it is easy to show that the probability that

the power of an OFDM signal component $x(n)$ is smaller than $\gamma E\{|x(n)|^2\}$ is given as

$$\Gamma(\gamma) \triangleq P\left(\frac{|x(n)|^2}{E\{|x(n)|^2\}} < \gamma\right) = 1 - e^{-\gamma}.$$

Moreover, IFFT of statistically independent inputs produces statistically independent outputs and thus the OFDM signal components are mutually independent.

Also, we assume that U phase rotation vectors are mutually independent and thus U alternative OFDM signal sequences are mutually independent. Then, we have [31]

$$P(\text{PAPR}(\mathbf{x}^u) < \gamma) = \Gamma^N(\gamma).$$

5.1.3.2. Derivation of $K_N(b)$

Since D_N is defined as the computational complexity for one N-point IFFT and $N \log_2 N$ nodes have to be computed in one N-point IFFT, we can define the computational complexity per node as

$$d \triangleq \frac{D_N}{N \log_2 N}.$$

Then, as in Fig. 5.1, the first OFDM signal component $x(0)$ is generated by computing $(2^0 + 2^1 + 2^2)$ 'dashed circle' nodes, which requires the computational complexity $(2^0 + 2^1 + 2^2)d$. Similarly, the computational complexity to generate the first OFDM signal component $x(0)$ in an N-point IFFT by the sequential generation is $(2^0 + \cdots + 2^{\log_2 N - 1})d$ which corresponds to $K_N(1)$. In conclusion, the computational complexity

$K_N(b)$ to generate b OFDM signal components, $1 \leq b \leq N$, in an N-point IFFT by the sequential generation is obtained as

$$K_N(b) = (2^0 + \cdots + 2^{\log_2 N - 1})d + \Big(\Big\lfloor \frac{b-1}{2^0} \Big\rfloor \cdot 2^0 + \cdots + \Big\lfloor \frac{b-1}{2^{\log_2 N - 1}} \Big\rfloor \cdot 2^{\log_2 N - 1} \Big) d. \tag{5.2}$$

Note that, $K_N(N) = (N \log_2 N)d = D_N$.

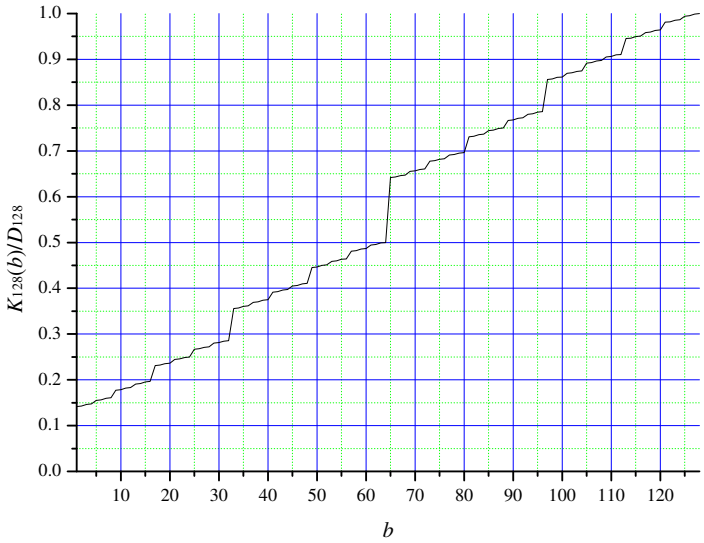

Figure 5.4: Relative computational complexity required to generate b OFDM signal components in an 128-point IFFT by the sequential generation.

In order to have an insight into the computational complexity, $K_N(b)/D_N$ versus b for $N = 128$ is plotted in Fig. 5.4. Note that the plot in Fig. 5.4 shows a near linear relationship. For instance, $b = 64$ at the x-axis corresponds to 0.5 at the y-axis, which implies that, by using the sequential generation, a half of OFDM signal components are generated with a half

of the computational complexity of one IFFT.

5.1.3.3. Distribution of $p_{B_u}(b_u)$

Clearly, the probability distribution of B_u depends on the value of $\gamma^{(u-1)}$ and thus the PMF of B_u can be represented as

$$p_{B_u}(b_u) = \int_1^{\infty} p_{B_u|\gamma^{(u-1)}}(b_u \mid \gamma)\ f_{\gamma^{(u-1)}}(\gamma)d\gamma \tag{5.3}$$

for an integer b_u within $[1, N]$, where $p_{B_u|\gamma^{(u-1)}}(b_u \mid \gamma)$ is the conditional PMF of B_u given that $\gamma^{(u-1)} = \gamma$ and $f_{\gamma^{(u-1)}}(\gamma)$ is the probability density function (PDF) of the random variable $\gamma^{(u-1)}$.

By using $\Gamma(\gamma)$, $p_{B_u|\gamma^{(u-1)}}(b_u \mid \gamma)$ and $f_{\gamma^{(u-1)}}(\gamma)$ are expressed [18] as

$$p_{B_u|\gamma^{(u-1)}}(b_u \mid \gamma) = \begin{cases} (1-\Gamma(\gamma))\Gamma^{b_u-1}(\gamma), & 1 \le b_u \le N-1 \\ \Gamma^{N-1}(\gamma), & b_u = N \end{cases} \tag{5.4}$$

and

$$\begin{aligned} f_{\gamma^{(u-1)}}(\gamma) &= \frac{d}{d\gamma}F_{\gamma^{(u-1)}}(\gamma) \\ &= \frac{d}{d\gamma}\Big(1 - \prod_{v=1}^{u-1} P(\mathrm{PAPR}(\mathbf{x}^v) > \gamma)\Big) \\ &= \frac{d}{d\gamma}(1-(1-\Gamma^N(\gamma))^{u-1}) \end{aligned} \tag{5.5}$$

where $F_{\gamma^{(u-1)}}(\gamma)$ is the cumulative distribution function (CDF) of $\gamma^{(u-1)}$. Therefore, by plugging (5.2) and (5.3) into (5.1), we obtain the average computational complexity of the conventional SLM scheme aided by the ES method for Nyquist sampling case.

5.1.4. Complexity Analysis for Oversampling Case

Practically, SLM schemes are often used with four-times oversampling to estimate the PAPR more accurately. In this subsection, we analyze the computational complexity of the conventional SLM scheme aided by the ES method for four-times oversampling case. In the conventional SLM scheme, the four-times oversampled alternative OFDM signal sequence is generated by performing $4N$-point IFFT to the input symbol sequence of length N padded with $3N$ zeroes.

Let B_u be the random variable representing the number of generated oversampled OFDM signal components at the u-th IFFT in the conventional SLM scheme aided by the ES method and its range is $[1, 4N]$. Thus, similar to the Nyquist sampling case, the average computational complexity of the conventional SLM scheme aided by the ES method for four-times oversampling case is

$$D_{4N} + \sum_{b_2=1}^{4N} K_{4N}(b_2) p_{B_2}(b_2) + \cdots + \sum_{b_U=1}^{4N} K_{4N}(b_U) p_{B_U}(b_U)$$

where $K_{4N}(b)$ denotes the computational complexity to generate b OFDM signal components, $1 \leq b \leq 4N$, in a $4N$-point IFFT by the sequential generation and $p_{B_u}(b_u)$ is the PMF of B_u.

5.1.4.1. Characteristics of a Four-Times Oversampled OFDM Signal Sequence

Let $\tilde{\mathbf{x}}^u = [\tilde{x}^u(0), \tilde{x}^u(1), \cdots, \tilde{x}^u(4N-1)]^T$ denote the u-th four-times oversampled alternative OFDM signal sequence and let $E\{|\tilde{x}(n)|^2\} = 2\sigma^2$.

Now we introduce several characteristics of the four-times oversampled OFDM signal components. Firstly, since the distribution of $\mathrm{PAPR}(\tilde{\mathbf{x}}^u)$ is similar to that of continuous OFDM signal, the CDF of $\mathrm{PAPR}(\tilde{\mathbf{x}}^u)$ can be approximated by using the results for the continuous OFDM signal in [31] as

$$P(\mathrm{PAPR}(\tilde{\mathbf{x}}^u) < \gamma) \simeq \exp\Big\{ - e^{-\gamma} N \sqrt{\frac{\pi}{3} \ln N} \Big\}. \tag{5.6}$$

Secondly, the four-times oversampled OFDM signal components $\tilde{x}(n)$ can be regarded as complex Gaussian random variables with zero mean and variance $2\sigma^2$ from the central limit theorem. Thirdly, from Appendix A, when the sequential generation is used, the four-times oversampled OFDM signal components are generated in the following order.

$$\{\tilde{x}(4s) : s \in \mathbb{Z}_N\} \to \{\tilde{x}(4s+2) : s \in \mathbb{Z}_N\}$$
$$\to \{\tilde{x}(4s+1) : s \in \mathbb{Z}_N\} \to \{\tilde{x}(4s+3) : s \in \mathbb{Z}_N\}.$$

Fourthly, from Appendix B, the four-times oversampled OFDM signal components in the same set $\{\tilde{x}(4s+p) : s \in \mathbb{Z}_N\}$ for any fixed $p \in \mathbb{Z}_4$ are statistically independent.

5.1.4.2. Derivation of $K_{4N}(b)$

Clearly, $K_{4N}(b)$ is the function obtained by replacing N of $K_N(b)$ in (5.2) by $4N$.

5.1.4.3. Distribution of $p_{B_u}(b_u)$

Similar to the Nyquist sampling case, $p_{B_u}(b_u)$ is represented as

$$p_{B_u}(b_u) = \int_1^{\infty} p_{B_u|\gamma^{(u-1)}}(b_u \mid \gamma)\ f_{\gamma^{(u-1)}}(\gamma)d\gamma \tag{5.7}$$

for an integer b_u in $[1, 4N]$.

Using (5.6), the PDF $f_{\gamma^{(u-1)}}(\gamma)$ in (5.7) is given as

$$\begin{aligned} f_{\gamma^{(u-1)}}(\gamma) &= \frac{d}{d\gamma}F_{\gamma^{(u-1)}}(\gamma) \\ &= \frac{d}{d\gamma}\Big(1 - \prod_{v=1}^{u-1} P(\mathrm{PAPR}(\tilde{\mathbf{x}}^v) > \gamma)\Big) \\ &= \frac{d}{d\gamma}\Big(1 - \Big(1 - \exp\Big\{ - e^{-\gamma} N\sqrt{\frac{\pi}{3}\ln N}\Big\}\Big)^{u-1}\Big). \end{aligned}$$

Using the characteristics of the four-times oversampled OFDM signal components $\tilde{x}(n)$, the conditional PMF $p_{B_u|\gamma^{(u-1)}}(b_u \mid \gamma)$ in (5.7) is given as

$$p_{B_u|\gamma^{(u-1)}}(b_u \mid \gamma)$$

$$= \begin{cases} (1-\Gamma(\gamma))\Gamma^{b_u-1}(\gamma), & 1 \le b_u \le N \\ (1-\Upsilon(\gamma))\Upsilon^{b_u-N-1}(\gamma)\Gamma^N(\gamma), & N+1 \le b_u \le 2N \\ (1-\Psi(\gamma))\Psi^{b_u-2N-1}(\gamma)\Upsilon^N(\gamma)\Gamma^N(\gamma), & 2N+1 \le b_u \le 3N \\ (1-\Phi(\gamma))\Phi^{b_u-3N-1}(\gamma)\Psi^N(\gamma)\Upsilon^N(\gamma)\Gamma^N(\gamma), & 3N+1 \le b_u \le 4N-1 \\ \Phi^{N-1}(\gamma)\Psi^N(\gamma)\Upsilon^N(\gamma)\Gamma^N(\gamma), & b_u = 4N \end{cases}$$

where

$$\begin{aligned}
\Gamma(\gamma) =& P(|\tilde{x}(4m)|^2 < 2\sigma^2\gamma) = 1 - e^{-\gamma} \\
\Upsilon(\gamma) =& P(|\tilde{x}(4m+2)|^2 < 2\sigma^2\gamma \mid |\tilde{x}(4s)|^2 < 2\sigma^2\gamma \ \forall \ s \in \mathbb{Z}_N) \\
\Psi(\gamma) =& P(|\tilde{x}(4m+1)|^2 < 2\sigma^2\gamma \mid |\tilde{x}(4s)|^2, |\tilde{x}(4s+2)|^2 < 2\sigma^2\gamma \ \forall \ s \in \mathbb{Z}_N) \\
\Phi(\gamma) =& P(|\tilde{x}(4m+3)|^2 < 2\sigma^2\gamma \mid |\tilde{x}(4s)|^2, \\
& |\tilde{x}(4s+1)|^2, |\tilde{x}(4s+2)|^2 < 2\sigma^2\gamma \ \forall \ s \in \mathbb{Z}_N)
\end{aligned} \tag{5.8}$$

for $m \in \mathbb{Z}_N$.

Since the oversampled OFDM signal components $\tilde{x}(n)$ are complex Gaussian random variables, $\Upsilon(\gamma)$,$\Psi(\gamma)$, and $\Phi(\gamma)$ in (5.8) are obtained by dealing with joint Gaussian PDFs. We only derive $\Upsilon(\gamma)$ in Appendix C due to the lack of space and $\Psi(\gamma)$ and $\Phi(\gamma)$ can be analogously obtained.

5.1.5. Comparison between Analytical and Simulation Results

In this subsection, we compare the analytical results in Sections 5.1.3 and 5.1.4 and the simulation results obtained by simulating 10^5 randomly generated input symbol sequences with 16-QAM for each subcarrier. Since the distribution of $p_{B_u}(b_u)$ for Nyquist sampling and four-times oversampling cases in (5.3) and (5.7) are too complex to deal with, numerical integration and least squares curve fitting of $\Upsilon(\gamma)$,$\Psi(\gamma)$, and $\Phi(\gamma)$ in (5.8) are utilized to obtain analytical results. The number of subcarriers is $N = 256$ and the numbers of the alternative OFDM signal sequences are $U = 2, 3, \cdots, 10$.

The CCRR is used to evaluate the computational benefit of the proposed ES method. The CCRR of the conventional SLM scheme aided by the proposed ES method over the conventional SLM scheme is defined as

$$\left(1 - \frac{\text{complexity of the conventional SLM aided by ES}}{\text{complexity of the conventional SLM without ES}}\right) \times 100\ (\%). \tag{5.9}$$

CCRR for other SLM schemes can be similarly defined.

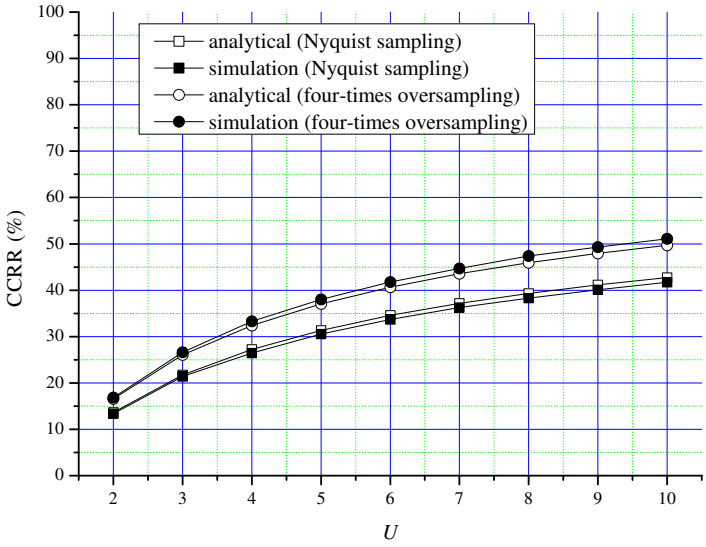

Figure 5.5: Comparison between the analytical and the simulation results using CCRR of the conventional SLM scheme aided by the proposed ES method over the conventional SLM scheme when $N = 256$.

Fig. 5.5 compares the analytical and the simulation results in terms of CCRR of the conventional SLM scheme aided by the proposed ES method over the conventional SLM scheme as a function of U for the two sampling

cases. In Fig. 5.5, for both sampling cases, the analytical results derived in Sections 5.1.3 and 5.1.4 show very good agreement with the simulation results. As U increases, small gap appears between the two results, which may be due to the several assumptions in the derivations.

5.2. Application of the ES Method to Various Low-Complexity SLM Schemes

In this section, we briefly introduce how to apply the proposed ES method to Lim's [25], Wang's [22], and Baxley's [27] low-complexity SLM schemes. The basic methodology of these applications is similar to the conventional SLM case. In Lim's, Wang's, and Baxely's SLM schemes, it is possible to implement the sequential generation of the alternative OFDM signal components and thus the ES method can be applied to these SLM schemes. Note that the ES method can be applied to other SLM schemes if the sequential generation is possible.

5.2.1. Lim's SLM Scheme Aided by the ES Method

In Lim's SLM scheme aided by the ES method, the common IFFT procedure from the 1-st stage to the $(\log_2 N - r)$-th stage is the same as the case without the ES method. However, at the remaining stages of IFFT, the sequential generation can be implemented similarly to the result in Section 5.1.1. Consequently, to generate the $U - 1$ alternative OFDM signal sequences, the remaining stages can be partially processed based on the intermediate minimum PAPR value.

5.2.2. Wang's SLM Scheme Aided by the ES Method

Clearly, some part of an alternative OFDM signal sequence is generated by multiplying the corresponding columns of the conversion matrix to the original OFDM signal sequence $\mathbf{x}$. Thus, the sequential generation can be implemented in Wang's SLM scheme. Consequently, the $U-1$ conversion matrix-vector multiplications can be partially processed based on the intermediate minimum PAPR value.

5.2.3. Baxely's SLM Scheme Aided by the ES Method

Baxely's SLM scheme uses the saturation PAPR point of HPA as γ_0. Therefore, if the ES method is applied, each IFFT is partially processed based on γ_0. More precisely, while the alternative OFDM signal components are sequentially generated by performing IFFT, the generation can be interrupted if an OFDM signal component having a power larger than $\gamma_0 E\{|x(n)|^2\}$ appears. Then, the next alternative OFDM signal sequence is sequentially generated and checked by γ_0 in the same manner.

As mentioned earlier, all the U alternative OFDM signal sequences have larger PAPR values than γ_0 with very low probability, for example, such probability value is 1.37×10^{-7} for $N = 256$, $U = 16$, and $\gamma_0 = 8$dB. When all U alternative OFDM signal sequences have larger PAPR than γ_0, Baxely's SLM scheme without the ES method tests all the U alternative OFDM signal sequences and selects the one with the minimum PAPR which is larger than γ_0. Likewise, in this case, Baxely's SLM scheme with the ES method finishes all the partially processed U IFFT blocks and

selects the one with the minimum PAPR. The computational complexity of three low-complexity SLM schemes aided by the ES method can be analytically derived in the analogous manner as in Sections 5.1.3 and 5.1.4.

5.3. Simulation Results

In this section, we present some numerical results including the average computational complexity given by simulating 10^5 randomly generated input symbol sequences. As in other literatures, we only compare the computational complexity required for generation of alternative OFDM signal sequences, which is a dominant factor in SLM schemes. Clearly, the PAPR reduction performance is not degraded by applying the ES method and thus we compare only the computational complexity. The computational benefit of the ES method does not depend on the modulation order and thus 16-QAM is used for all cases.

5.3.1. Simulation Results for the Conventional SLM Scheme Aided by the ES Method

For the conventional SLM case, we simulate the OFDM system with $N = 256,\ 1024$. Table 5.1 provides the computational complexity and the CCRR of the conventional SLM scheme aided by the ES method over the conventional SLM scheme for two sampling cases. To implement four-times oversampling, $3N$ zeroes are added to the (alternative) input symbol sequences and $4N$-point IFFT is performed. Therefore, the computational complexity of the conventional SLM scheme without the ES

method is UD_{4N} when four-times oversampling is used. Table 5.1 shows that the ES method substantially reduces the computational complexity of the conventional SLM scheme for all cases. Table 5.1 also shows that the number of subcarriers N has little effect on the computational benefit of the ES method. Also, the reduction ratio of computational complexity by using the ES method increases as U increases.

Table 5.1: Computational Benefit of the Conventional SLM Scheme Aided by the ES Method

Sampling	N	Scheme	$U = 8$	$U = 16$	$U = 32$
Nyquist sampling	256	Conv. SLM w/o ES	8 D_N	16 D_N	32 D_N
		Conv. SLM w/ ES	4.92 D_N	8.31 D_N	14.26 D_N
		CCRR (%)	38.5	48.1	55.4
	1024	Conv. SLM w/o ES	8 D_N	16 D_N	32 D_N
		Conv. SLM w/ ES	4.81 D_N	8.03 D_N	13.58 D_N
		CCRR (%)	39.9	49.8	57.6
Four-times oversampling	256	Conv. SLM w/o ES	8 D_{4N}	16 D_{4N}	32 D_{4N}
		Conv. SLM w/ ES	4.21 D_{4N}	6.69 D_{4N}	10.82 D_{4N}
		CCRR (%)	47.4	58.2	66.2
	1024	Conv. SLM w/o ES	8 D_{4N}	16 D_{4N}	32 D_{4N}
		Conv. SLM w/ ES	4.22 D_{4N}	6.65 D_{4N}	10.70 D_{4N}
		CCRR (%)	47.3	58.4	66.6

5.3.2. Simulation Results for Low-Complexity SLM Schemes Aided by the ES Method

For the three low-complexity SLM schemes introduced earlier, simulation has been performed when $N = 256$ and four-times oversampling is used.

Table 5.2 shows the computational complexity and the CCRR of the Lim's SLM scheme aided by the ES method over Lim's SLM scheme. In Lim's SLM scheme, the number of remaining stages r is set to 5 guaranteeing good PAPR reduction performance. It is clear that the ES method substantially reduces the computational complexity of Lim's SLM scheme.

Table 5.2: Computational Benefit of the ES Method for Lim's SLM Scheme

	$U = 8$	$U = 16$	$U = 32$
Lim's SLM w/o ES	4.5 D_{4N}	8.5 D_{4N}	16.5 D_{4N}
Lim's SLM w/ ES	2.46 D_{4N}	3.48 D_{4N}	5.10 D_{4N}
CCRR (%)	45.3	59.1	69.1

Table 5.3 shows the computational complexity and the CCRR of the Wang's SLM scheme aided by the ES method over Wang's SLM scheme. In Table 5.3, the complexity is measured by using the comparison of the number of complex additions required for conversion matrix-vector multiplications in Wang's SLM scheme. Since Wang's SLM scheme has a constraint on U, the cases of $U = 4, 8, 12$ are simulated. We can see that the ES method substantially reduces the computational complexity of Wang's SLM scheme.

Table 5.4 shows the computational complexity and the CCRR of the Baxely's SLM scheme aided by the ES method over Baxley's SLM scheme. For simplicity, the number of alternative OFDM signal sequences is fixed to $U = 16$. In Table 5.4, we can see that the computational benefit of the ES method depends on the value of γ_0, the saturation PAPR point of

Table 5.3: Computational Benefit of the ES Method for Wang's SLM Scheme

	$U = 4$	$U = 8$	$U = 12$
Wang's SLM w/o ES	9,216 com. add.	21,504 com. add.	33,792 com. add.
Wang's SLM w/ ES	4,933 com. add.	9,288 com. add.	12,820 com. add.
CCRR (%)	46.5	56.8	62.1

HPA.

Table 5.4: Computational Benefit of the ES Method for Baxely's SLM Scheme

	$\gamma_0 = 7.5$dB	$\gamma_0 = 8.0$dB	$\gamma_0 = 8.5$dB
Baxely's SLM scheme w/o ES	8.03 D_{4N}	3.24 D_{4N}	1.73 D_{4N}
Baxely's SLM scheme w/ ES	5.12 D_{4N}	1.81 D_{4N}	1.28 D_{4N}
CCRR (%)	36.2	44.1	26.1

Note that even for the low-complexity SLM schemes the ES method provides large computational benefit. That is, the ES method can be effectively combined with almost all the existing SLM schemes to further reduce the computational complexity.

5.4. Conclusions

When various SLM schemes generate alternative OFDM signal sequences, the proposed ES method selects the transmitted OFDM signal sequence efficiently. Aided by the ES method, the alternative OFDM signal components are sequentially generated and the generation procedure can be interrupted according to the component power value. As a result, the average computational complexity of the SLM schemes is substantially

reduced. It is meaningful to mention that the application of the proposed ES method does not degrade the PAPR reduction performance of the used SLM scheme.

In this chapter, we described how to apply the ES method to the conventional SLM scheme and analyzed its computational complexity. Furthermore, we briefly described the application of the proposed ES method to the three previously low-complexity SLM schemes, and simulation results confirmed the computational benefit of the ES method. We anticipate that the proposed ES method can be effectively applied to many other SLM schemes beyond the SLM schemes described in this chapter.

Appendix A

We will show that the sequential generation in Section 5.1.1 generates the four-times oversampled OFDM signal components in the order as

$$\{\tilde{x}(4s) : s \in \mathbb{Z}_N\} \rightarrow \{\tilde{x}(4s+2) : s \in \mathbb{Z}_N\}$$
$$\rightarrow \{\tilde{x}(4s+1) : s \in \mathbb{Z}_N\} \rightarrow \{\tilde{x}(4s+3) : s \in \mathbb{Z}_N\}.$$

The sequential generation in Section 5.1.1 uses a DIT FFT structure and thus generates $4N$ oversampled OFDM signal components in *bit-reversed* order as

$$\tilde{x}((\underbrace{000\cdots00}_{\log_2 N+2 \text{ bits}})_2) \rightarrow \tilde{x}((\underbrace{100\cdots00}_{\log_2 N+2 \text{ bits}})_2)$$
$$\rightarrow \tilde{x}((\underbrace{010\cdots00}_{\log_2 N+2 \text{ bits}})_2) \rightarrow \cdots \rightarrow \tilde{x}((\underbrace{111\cdots11}_{\log_2 N+2 \text{ bits}})_2)$$

where $(\cdot)_2$ denotes the binary representation of integer number.

Then, the generation order of components is easily divided into

$$\underbrace{\tilde{x}((\underbrace{00\cdots0}_{\log_2 N \text{ bits}}\ 00)_2) \to \tilde{x}((\underbrace{01\cdots0}_{\log_2 N \text{ bits}}\ 00)_2) \to \cdots \to \tilde{x}((\underbrace{11\cdots1}_{\log_2 N \text{ bits}}\ 00)_2)}_{\{\tilde{x}(4s):s\in\mathbb{Z}_N\}}$$

$$\to \underbrace{\tilde{x}((\underbrace{00\cdots0}_{\log_2 N \text{ bits}}\ 10)_2) \to \tilde{x}((\underbrace{01\cdots0}_{\log_2 N \text{ bits}}\ 10)_2) \to \cdots \to \tilde{x}((\underbrace{11\cdots1}_{\log_2 N \text{ bits}}\ 10)_2)}_{\{\tilde{x}(4s+2):s\in\mathbb{Z}_N\}}$$

$$\to \underbrace{\tilde{x}((\underbrace{00\cdots0}_{\log_2 N \text{ bits}}\ 01)_2) \to \tilde{x}((\underbrace{01\cdots0}_{\log_2 N \text{ bits}}\ 01)_2) \to \cdots \to \tilde{x}((\underbrace{11\cdots1}_{\log_2 N \text{ bits}}\ 01)_2}_{\{\tilde{x}(4s+1):s\in\mathbb{Z}_N\}}$$

$$\to \underbrace{\tilde{x}((\underbrace{00\cdots0}_{\log_2 N \text{ bits}}\ 11)_2) \to \tilde{x}((\underbrace{01\cdots0}_{\log_2 N \text{ bits}}\ 11)_2) \to \cdots \to \tilde{x}((\underbrace{11\cdots1}_{\log_2 N \text{ bits}}\ 11)_2}_{\{\tilde{x}(4s+3):s\in\mathbb{Z}_N\}}.$$

Appendix B

We want to show that when four-times oversampling is used, the oversampled OFDM signal components in the same set $\{\tilde{x}(4s+p) : s \in \mathbb{Z}_N\}$ for any fixed $p \in \mathbb{Z}_4$ are statistically independent.

Four-times oversampled OFDM signal components are generated by the $4N$-point IFFT of the zero-padded input symbol sequence given as

$$\{X(0), X(1), \cdots, X(\frac{N}{2}-1), \underbrace{0, 0, \cdots, 0}_{3N \text{ zeroes}}, X(\frac{N}{2}), X(\frac{N}{2}+1), \cdots, X(N-1)\}.$$

Thus the four-times oversampled OFDM signal component $\tilde{x}(4s+p)$ is

expressed as

$$\begin{aligned}\tilde{x}(4s+p) &= \sum_{k=0}^{\frac{N}{2}-1} X(k)e^{j\frac{2\pi}{4N}k(4s+p)} + \sum_{k=\frac{7N}{2}}^{4N-1} X(k-3N)e^{j\frac{2\pi}{4N}k(4s+p)} \\ &= \sum_{k=0}^{\frac{N}{2}-1} X(k)e^{j\frac{2\pi}{4N}kp}e^{j\frac{2\pi}{N}ks} + \sum_{k=\frac{N}{2}}^{N-1} X(k)e^{j\frac{2\pi}{4N}(k+3N)p}e^{j\frac{2\pi}{N}ks} \\ &= \sum_{k=0}^{N-1} X'(k)e^{j\frac{2\pi}{N}ks}\end{aligned}$$

where

$$X'(k) = \begin{cases} X(k)e^{j\frac{2\pi}{4N}kp}, & 0 \le k \le \frac{N}{2}-1 \\ X(k)e^{j\frac{2\pi}{4N}(k+3N)p}, & \frac{N}{2} \le k \le N-1. \end{cases}$$

It is well known that IFFT of statistically independent inputs also produces statistically independent outputs [31]. Since the components in $\{\tilde{x}(4s+p) : s \in \mathbb{Z}_N\}$ for any fixed p are the outputs of N-point IFFT whose inputs are statistically independent random variables $X'(k)$, the components in the set $\{\tilde{x}(4s+p) : s \in \mathbb{Z}_N\}$ for any fixed $p \in \mathbb{Z}_4$ are statistically independent.

Appendix C

We will derive the function $\Upsilon(\gamma)$ in (5.8). Since a four-times oversampled OFDM signal component $\tilde{x}(n)$ has large correlation with its neighboring components, $\Upsilon(\gamma)$ can be approximated as

$$\begin{aligned}\Upsilon(\gamma) &= P(|\tilde{x}(4m+2)|^2 < 2\sigma^2\gamma \mid |\tilde{x}(4s)|^2 < 2\sigma^2\gamma \ \forall\ s \in \mathbb{Z}_N) \\ &\simeq P(|\tilde{x}(4m+2)|^2 < 2\sigma^2\gamma \mid |\tilde{x}(4m)|^2,\ |\tilde{x}(4m+4)|^2 < 2\sigma^2\gamma)\end{aligned}$$

$$= \frac{P(|\tilde{x}(4m)|^2,\ |\tilde{x}(4m+2)|^2,\ |\tilde{x}(4m+4)|^2 < 2\sigma^2\gamma)}{\Gamma^2(\gamma)}. \qquad (5.10)$$

In (5.10), the oversampled OFDM signal components $\tilde{x}(4m)$, $\tilde{x}(4m+2)$, and $\tilde{x}(4m+4)$ are jointly complex Gaussian random variables, each with zero mean and variance $2\sigma^2$. Let I_p and Q_p denote the in-phase and quadrature components of $\tilde{x}(4m+p)$, respectively, and then the joint PDF of I_0, I_2, I_4, Q_0, Q_2, and Q_4 is given as

$$f_{I_0 I_2 I_4 Q_0 Q_2 Q_4}(\mathbf{z}) = \frac{1}{\sqrt{(2\pi)^6 |\mathbf{\Sigma}|}} \exp\{-\frac{1}{2}\ \mathbf{z}\ \mathbf{\Sigma}^{-1}\ \mathbf{z}^T\} \qquad (5.11)$$

where

$$\mathbf{z} = [i_0, i_2, i_4, q_0, q_2, q_4]$$

and $\mathbf{\Sigma}$ is the covariance matrix of Gaussian random vector $\mathbf{z}$.

Firstly, I_p and Q_p are uncorrelated for all p's. Secondly, $\mathrm{cov}(I_0, I_4) = \mathrm{cov}(Q_0, Q_4) = 0$ from Appendix B where $\mathrm{cov}(a, b)$ means the covariance between a and b. It is known that four-times oversampling can be implemented by using low pass filter whose impulse response is the sinc function [41]. That is, $\tilde{x}(4m+2)$ can be represented by an infinite series as

$$\begin{aligned}\tilde{x}(4m+2) =& \mathrm{sinc}(\frac{\pi}{2})\tilde{x}(4m) + \mathrm{sinc}(\frac{\pi}{2})\tilde{x}(4m+4) \\ &+ \mathrm{sinc}(\frac{3\pi}{2})\tilde{x}(4m-4) + \mathrm{sinc}(\frac{3\pi}{2})\tilde{x}(4m+8) + \cdots\end{aligned}$$

where $\mathrm{sinc}(x) = \sin(x)/x$ and the oversampled OFDM signal components $\tilde{x}(4s)$ for all $s \in \mathbb{Z}_N$ are statistically independent from Appendix B. Thus,

we have

$$\mathrm{cov}(I_0, I_2) = \mathrm{cov}(I_2, I_4) = \mathrm{cov}(Q_0, Q_2) = \mathrm{cov}(Q_2, Q_4) \approx \mathrm{sinc}(\frac{\pi}{2})\sigma^2.$$

Conclusively, the covariance matrix $\mathbf{\Sigma}$ is approximated as

$$\mathbf{\Sigma} \approx \begin{pmatrix} \sigma^2 & \mathrm{sinc}(\frac{\pi}{2})\sigma^2 & 0 & 0 & 0 & 0 \\ \mathrm{sinc}(\frac{\pi}{2})\sigma^2 & \sigma^2 & \mathrm{sinc}(\frac{\pi}{2})\sigma^2 & 0 & 0 & 0 \\ 0 & \mathrm{sinc}(\frac{\pi}{2})\sigma^2 & \sigma^2 & 0 & 0 & 0 \\ 0 & 0 & 0 & \sigma^2 & \mathrm{sinc}(\frac{\pi}{2})\sigma^2 & 0 \\ 0 & 0 & 0 & \mathrm{sinc}(\frac{\pi}{2})\sigma^2 & \sigma^2 & \mathrm{sinc}(\frac{\pi}{2})\sigma^2 \\ 0 & 0 & 0 & 0 & \mathrm{sinc}(\frac{\pi}{2})\sigma^2 & \sigma^2 \end{pmatrix}. \tag{5.12}$$

By changing the variables of the joint PDF in (5.11) into polar forms and using it, $\Upsilon(\gamma)$ in (5.10) can be expressed as

$$\begin{aligned} \Upsilon(\gamma) = \Bigg(& \int_0^{\sqrt{2\sigma^2\gamma}} \int_0^{\sqrt{2\sigma^2\gamma}} \int_0^{\sqrt{2\sigma^2\gamma}} \int_0^{2\pi} \int_0^{2\pi} \int_0^{2\pi} \\ & f_{I_0 I_2 I_4 Q_0 Q_2 Q_4}(r_0\cos(\theta_0), r_2\cos(\theta_2), r_4\cos(\theta_4), \\ & r_0\sin(\theta_0), r_2\sin(\theta_2), r_4\sin(\theta_4)) \\ & r_0\ r_2\ r_4\ d\theta_0\ d\theta_2\ d\theta_4\ dr_0\ dr_2\ dr_4 \Bigg) / (1 - e^{-\gamma})^2. \end{aligned}$$

Chapter 6. Clipping Noise Cancellation for OFDM Systems Using Reliable Observations Based on Compressed Sensing

Clipping is the simplest way to reduce PAPR of OFDM signals and thus has been widely studied [7], [8], [33]–[36]. Clipping at the Nyquist sampling rate has been used for low-complexity applications but suffers from peak regrowth after D/A conversion. It is known that clipping an oversampled OFDM signal reduces the peak regrowth after D/A conversion, but it causes out-of-band radiation which has to be filtered [7]. The distortion of the OFDM signal caused by clipping is called clipping noise which has sparsity in time domain. There are several schemes to mitigate clipping noise [37], [38], [42]–[45], among which the scheme in [37] performs iterative ML estimation for all tones and recreates clipping procedure in order to reconstruct clipping noise.

According to recent results in sparse signal processing, also known as compressed sensing (CS) theory [46]–[49], a sparse signal can be reconstructed from its compressed observations. In this context, clipping noise can be effectively reconstructed at the receiver by CS reconstruction algorithms. As the first work for this, a tone reservation scheme using CS is proposed in [28], where several tones are reserved at the transmitter before

clipping, and the receiver reconstructs the clipping noise by exploiting the compressed observations of the reserved tones. However, in this scheme, the reserved tones induce data rate loss and due to the vulnerability of CS reconstruction algorithms to the channel noise BER performance is poor. Another clipping noise cancellation scheme using CS is proposed in [29], motivated by the results in [28]. The scheme in [29] does not induce data rate loss because the compressed observations of the pilot tones are exploited. However, it still shows poor BER performance due to its vulnerability to the channel noise.

In this chapter, we propose a new clipping noise cancellation scheme using CS, which selectively uses observations of data tones. That is, reliable observations contaminated by less channel noise are selected and then the clipping noise is reconstructed from these compressed observations by using a CS reconstruction algorithm. The proposed scheme has the following three major advantages compared to the schemes in [28] and [29].

- In contrast with the scheme in [28], the proposed scheme does not reserve tones and instead exploits compressed observations of the underlying clipping noise in data tones, which leads to no data rate loss.

- In practice, some OFDM systems do not insert pilot tones into every OFDM signal. Even in this case, the proposed scheme works well in contrast with the scheme in [29], which exploits pilot tones.

- The biggest difference is that the schemes in [28] and [29] use all the compressed observations without considering the reliability of observations, which may result in including the observations severely contaminated by the channel noise and thus it leads to inaccurate reconstruction of the clipping noise. However, the proposed scheme selects the observations less contaminated by the channel noise in order to utilize reliable compressed observations. By doing this, we successfully overcome the vulnerability of CS reconstruction to the channel noise. Note that the simulation results in Section 6.3 show that the proposed scheme mitigates the clipping noise well over both an AWGN channel and a Rayleigh fading channel.

Also, the authors in [51] proposed a clipping noise cancellation scheme exploiting reliable observations of data tones, which can be viewed as a contemporary work with our work. The basic idea of the data aided CS is common. However, the approach in [51] is entirely different from our approach.

Firstly, to improve the performance, we exploit a statistical model for a clipped signal derived by using the Bussgang's theorem. But, the scheme in [51] is based on a naive assumption on a clipped signal. In [51], the clipping noise in frequency domain is modeled as complex Gaussian. Secondly, we consider not only the clipping at the Nyquist sampling rate but also the clipping and filtering at an oversampling rate. The scheme in [51] only considers the former case. Note that the latter has been widely studied because it mitigates the peak regrowth after D/A conversion. Thirdly,

the scheme in [51] needs optimization of the number of compressed observations for a given signal-to-noise ratio (SNR) point, while our scheme needs no optimization process. Finally, the scheme in [51] only considers the decision error probability of received symbols to measure the reliability of observations, while we also consider a level of channel noise. Due to these differences, our scheme shows superior BER performance than the scheme in [51] as shown in simulation results in Section 6.3.

This chapter is organized as follows. CS is reviewed in Section 6.1 and a new clipping noise cancellation scheme is proposed in Section 6.2. Section 6.3 presents simulation results and conclusion is given in Section 6.4.

6.1. Preliminaries

6.1.1. Notation

Upper and lower case letters denote signals in frequency domain and signals in time domain, respectively. The $n+1$-th component of a column vector $\mathbf{x}$ is denoted as $x(n)$ and bold face letters denote vectors and matrices. $||\cdot||_0$, $||\cdot||_1$, and $||\cdot||_2$ indicate l_0-norm (the number of nonzero elements), l_1-norm, and l_2-norm, respectively.

6.1.2. Compressed Sensing

In a typical CS problem, the goal is to reconstruct an $N \times 1$ *K-sparse signal vector* $\mathbf{c}$ from an $M \times 1$ *compressed observation vector* $\tilde{\mathbf{Y}}$ under the condition $K \ll M < N$ [46]–[49]. A signal vector $\mathbf{c}$ is called K-sparse when it has at most K nonzeros, i.e., $||\mathbf{c}||_0 \leq K$. Then, $\mathbf{c}$ and $\tilde{\mathbf{Y}}$ are

linearly related to each other as

$$\tilde{\mathbf{Y}} = \mathbf{\Phi c} + \eta \tag{6.1}$$

where $\mathbf{\Phi}$ is an $M \times N$ *sensing matrix* and η is the $M \times 1$ *observation noise vector* with a bounded noise level $||\eta||_2 \leq \epsilon$.

To reconstruct $\mathbf{c}$, the following l_1-norm minimization problem, also known as basis pursuit (BP), to obtain $\hat{\mathbf{c}}$ is considered [47] as

$$\begin{aligned} &\arg \min_{||\mathbf{c}||_0 \leq K} \quad ||\mathbf{c}||_1 \\ &\text{subject to} \quad ||\mathbf{\Phi c} - \tilde{\mathbf{Y}}||_2 \leq \epsilon. \end{aligned} \tag{6.2}$$

It is shown that if the vector $\mathbf{c}$ is sufficiently sparse, then the solution $\hat{\mathbf{c}}$ in (6.2) is close to the true solution $\mathbf{c}$ within the noise level such as

$$||\mathbf{c} - \hat{\mathbf{c}}||_2 \leq O(1) \cdot \epsilon$$

when the sensing matrix $\mathbf{\Phi}$ satisfies a good restricted isometry property (RIP). In [47], a good RIP says that the matrix $\mathbf{\Phi}$ acts like an almost isometry on all K-sparse vectors $\mathbf{c}$.

Including a BP algorithm given in (6.2), a number of CS reconstruction algorithms have been proposed [46]–[48]. In this chapter, for comparison purpose, we adopt a sparse approximation algorithm called orthogonal matching pursuit (OMP) [52] because of its ease of implementation and speed. Note that OMP is a greedy algorithm which iteratively finds an index whose coefficient is thought to be nonzero based on correlation

calculation, and then those coefficients are estimated by least squares.

6.2. Clipping Noise Cancellation for OFDM Systems Based on CS

As mentioned in Section 3.1, the clipping procedure makes clipping noise $\mathbf{c}$ added to the OFDM signal sequence $\mathbf{x}$. In this section, we propose a clipping noise cancellation scheme for OFDM systems by using CS technique.

6.2.1. Sparsity of c

Due to the clipping (and filtering), the clipping noise $\mathbf{c}$ is added to the OFDM signal sequence $\mathbf{x}$ at the transmitter end. To recover and mitigate the clipping noise $\mathbf{c}$ by CS technique at the receiver, $\mathbf{c}$ needs to be sparse as much as possible.

6.2.1.1. Sparsity of c for Clipping at the Nyquist Sampling Rate

Let us denote the clipping ratio γ as in (3.2), and then the probability that $|x_1(n)| > A$ is $e^{-\gamma^2}$, due to the fact that the envelope of an OFDM signal sequence is Rayleigh distributed when N is sufficiently large. Also, $x_1(n)$ can be assumed to be i.i.d. random variables. Thus, the average number of nonzero elements in $\mathbf{c}$ is $N \cdot e^{-\gamma^2}$. Unless the clipping ratio γ is too small, the clipping noise $\mathbf{c}$ can be viewed as a sparse signal. For example, $E\{||\mathbf{c}||_0\} = N \cdot e^{-\gamma^2} \leq 0.184 \cdot N$ when $\gamma \geq 1.3 = 2.278$dB.

6.2.1.2. Sparsity of c for Clipping and Filtering at an Oversampling Rate

When $L > 1$, $\mathbf{c}$ is the $1/L$ downsampled version of the "filtered $\mathbf{c}_L$" of (3.3) and (3.5). Thus if the "filtered $\mathbf{c}_L$" has sparsity, $\mathbf{c}$ also inherits the sparsity. On the average, the number of nonzero elements in $\mathbf{c}$ is $1/L$ of that in $\mathbf{c}_L$. Thus we will investigate the sparsity of the filtered $\mathbf{c}_L$ denoted by $\mathbf{c}'_L$.

It is possible that the clipping noise is characterized as a series of parabolic pulses unless γ is too small [53]. The analysis in [53] is based on continuous-time signals, which can be easily extended to the discrete-time case because the oversampling factor L takes a value to make the discrete-time signals similar to the continuous-time signals. That is, the oversampled clipping noise $\mathbf{c}_L$ can be represented as

$$\mathbf{c}_L(n) = \sum_{i=1}^{N_p} f_i(n), \qquad 0 \le n \le LN - 1$$

where $f_i(n)$ is the i-th clipping parabolic pulse having its maximum amplitude at n_i and N_p is the number of the parabolic pulses. The average value of N_p is given as [53]

$$E\{N_p\} = N\sqrt{\frac{\pi}{3}}\gamma e^{-\gamma^2},$$

which is usually small one compared to N. For example, $E\{N_p\} \le 0.245 \cdot N$ when $\gamma \ge 1.3 = 2.278\text{dB}$.

Also, the filtered clipping noise vector $\mathbf{c}'_L$ can be represented as a sum

of N_p sinc functions as

$$c'_L(n) = \sum_{i=1}^{N_p} \alpha_i \cdot \mathrm{sinc}(\frac{\pi}{L}(n - n_i)), \qquad 0 \le n \le LN - 1$$

where α_i is a coefficient depending on the shape of $f_i(n)$.

Unfortunately, $\mathbf{c}'_L$ is not an exactly sparse signal, but most of its elements may be close to zero because the sinc function is a sine wave that decays in amplitude. The peak of the first sidelobe is only 21.22% of the peak of the mainlobe and the duration of the mainlobe is only $2L$. After downsampling $\mathbf{c}'_L$ to obtain $\mathbf{c}$ that we are interested in, the duration of the mainlobe of $\mathbf{c}$ is reduced to $2L/L = 2$. Such signals having mostly very small nonzero elements are called compressible, approximately sparse, or relatively sparse in various contexts [47], [54]. For approximately sparse case, it is known that CS techniques can be used to recover $\mathbf{c}$, which will be shown from the simulation results in Section 6.3.

6.2.2. Reconstruction of the Clipping Noise c by CS

In a matrix form, (3.11) can be rewritten as

$$\mathbf{H}^{-1}\mathbf{Y} = \bar{\mathbf{X}} + \mathbf{H}^{-1}\mathbf{Z} \tag{6.3}$$

where $\mathbf{H}$ is a diagonal matrix whose k-th diagonal element is $H(k)$ and $\mathbf{Y}$, $\bar{\mathbf{X}}$, and $\mathbf{Z}$ are $N \times 1$ column vectors. If we subtract $\hat{\mathbf{X}}$ in (3.12) from (6.3), we have

$$\mathbf{H}^{-1}\mathbf{Y} - \hat{\mathbf{X}} = \underbrace{\mathbf{C}}_{\text{noiseless observation vector}} + \underbrace{\mathbf{X} - \hat{\mathbf{X}} + \mathbf{H}^{-1}\mathbf{Z}}_{\text{observation noise vector}}$$

which is the sum of the noiseless observation vector and the observation noise vector.

It is obvious that if the whole observations (or whole tones) are used, reconstruction of the clipping noise $\mathbf{c}$ may be inaccurate due to the fact that some observations are severely contaminated by the observation noise. Therefore, our suggestion here is to select a reliable subset of the whole observations $\mathbf{H}^{-1}\mathbf{Y} - \hat{\mathbf{X}}$, namely M out of N components, and then we can obtain an $M \times 1$ compressed observation vector $\tilde{\mathbf{Y}}$. This process can be done by multiplying an $M \times N$ selection matrix $\mathbf{S}$ consisting of some M rows of $N \times N$ identity matrix $\mathbf{I}_N$. Such selection strategy will be described in the next subsection. Let $\mathbf{C} = \mathbf{F}\mathbf{c}$, where $\mathbf{F}$ is an $N \times N$ unitary discrete Fourier transform (DFT) matrix. Then we have

$$\begin{aligned}\tilde{\mathbf{Y}} = \mathbf{S}\mathbf{H}^{-1}\mathbf{Y} - \mathbf{S}\hat{\mathbf{X}} &= \mathbf{S}\mathbf{F}\mathbf{c} + \mathbf{S}(\mathbf{X} - \hat{\mathbf{X}}) + \mathbf{S}\mathbf{H}^{-1}\mathbf{Z} \\ &= \mathbf{\Phi}\mathbf{c} + \underbrace{\mathbf{S}(\mathbf{X} - \hat{\mathbf{X}}) + \mathbf{S}\mathbf{H}^{-1}\mathbf{Z}}_{\text{observation noise vector}} \\ &= \mathbf{\Phi}\mathbf{c} + \eta \end{aligned} \tag{6.4}$$

where the matrix $\mathbf{\Phi} = \mathbf{S}\mathbf{F}$ can be considered as the $M \times N$ *sensing matrix* from the view of CS. As one can see from [47], a sensing matrix for CS can be constructed by using a subset of rows in a DFT matrix, which shows a good RIP. Then (6.4) can be considered as a CS problem given in (6.1), where $\tilde{\mathbf{Y}}$ is the $M \times 1$ *compressed observation vector*, the clipping noise $\mathbf{c}$ is the $N \times 1$ *sparse signal vector*, and $\eta = \mathbf{S}(\mathbf{X} - \hat{\mathbf{X}}) + \mathbf{S}\mathbf{H}^{-1}\mathbf{Z}$ is the $M \times 1$ *observation noise vector*.

By using a CS recovery algorithm such as OMP, we can recover $\mathbf{c}$ denoted as $\hat{\mathbf{c}}$ from the compressed observation vector $\tilde{\mathbf{Y}}$ in (6.4). Then $\hat{\mathbf{C}} = \mathrm{FFT}_N(\hat{\mathbf{c}})$ is subtracted from the equalized received symbol sequence $\mathbf{H}^{-1}\mathbf{Y}$ and then the final decision $\hat{\mathbf{X}}_{\text{final}}$ is made as

$$\hat{\mathbf{X}}_{\text{final}}(k) = \arg\min_{s\in\mathcal{X}} |H^{-1}(k)Y(k) - \hat{C}(k) - s|.$$

Fig. 6.1 pictorially summarizes the proposed scheme, where $\mathbf{y}$ is the received OFDM signal sequence.

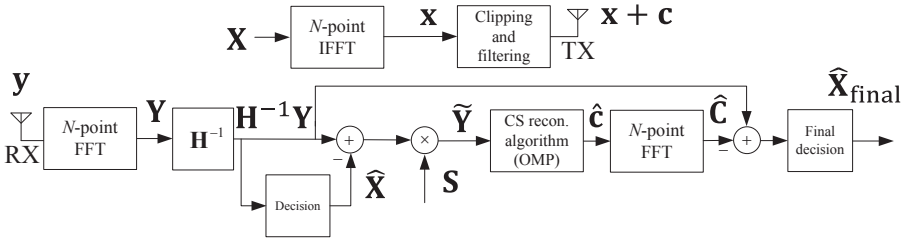

Figure 6.1: A block diagram of the proposed clipping noise cancellation scheme.

6.2.3. Construction of the Compressed Observation Vector $\tilde{\mathbf{Y}}$

As we already mentioned, the compressed observation vector can be obtained by selecting some reliable components of the whole observations $\mathbf{H}^{-1}\mathbf{Y} - \hat{\mathbf{X}}$ whose k-th component is given as

$$H^{-1}(k)Y(k) - \hat{X}(k) = \underbrace{C(k)}_{\text{noiseless observation}} + \underbrace{H^{-1}(k)Z(k) + X(k) - \hat{X}(k)}_{\text{observation noise}}. \tag{6.5}$$

6.2.3.1. Which Observations Should Be Selected?

The observations less contaminated by observation noise should be selected. For convenience, we will use $\theta(k)$ to denote the observation noise in (6.5) as

$$\theta(k) = H^{-1}(k)Z(k) + X(k) - \hat{X}(k).$$

That is, we have to select reliable observations which contain small $|\theta(k)|$.

6.2.3.2. Estimation of $\theta(k)$ Based on $H^{-1}(k)Y(k)$

In this subsubsection, we will derive the minimum mean square error (MMSE) estimator of $\theta(k)$, $\hat{\theta}(k)$. For convenience, we separate $\theta(k)$ into two parts, $\theta_0(k)$ and $\theta_1(k)$, as

$$\theta(k) = \underbrace{H^{-1}(k)Z(k)}_{\theta_0(k)} + \underbrace{X(k) - \hat{X}(k)}_{\theta_1(k)}.$$

Also, we treat the equalized received symbol $H^{-1}(k)Y(k)$ as observation $o(k)$ as

$$o(k) = H^{-1}(k)Y(k).$$

Then $\hat{\theta}(k)$ can be separately obtained by

$$\hat{\theta}(k) = E\{\theta(k) \mid o(k)\} = E\{\theta_0(k) \mid o(k)\} + E\{\theta_1(k) \mid o(k)\}.$$

For simplicity, we drop the subcarrier index k in the following derivation.

First, from (3.7) and (3.11), θ_0 is linearly related to observation o as

$$o = \theta_0 + \alpha X + D$$

and

$$\theta_0 \sim \mathcal{CN}(0, 2|H^{-1}|^2\sigma^2)$$
$$D \sim \mathcal{CN}(0, 2\sigma_D^2)$$
$$X = \mathcal{X}_i \text{ with probability } \frac{1}{|\mathcal{X}|}$$

where $\mathcal{X}_i$ denotes the i-th constellation point of signal constellation $\mathcal{X}$ and $|\mathcal{X}|$ denotes signal constellation size. We assume that each constellation point can be transmitted with equal probability.

Then, $E\{\theta_0 \mid o\}$ can be expressed as

$$\begin{aligned} E\{\theta_0 \mid o\} &= \int \theta_0 \; p(\theta_0 \mid o) \; d\theta_0 \\ &= \int \theta_0 \left(\sum_{X \in \mathcal{X}} p(\theta_0, X \mid o) \right) d\theta_0 \\ &= \int \theta_0 \left(\sum_{X \in \mathcal{X}} p(\theta_0 \mid X, o) \cdot p(X \mid o) \right) d\theta_0 \\ &= \sum_{X \in \mathcal{X}} \left(\int \theta_0 \; p(\theta_0 \mid X, o) \; d\theta_0 \right) \cdot p(X \mid o) \\ &= \sum_{X \in \mathcal{X}} E\{\theta_0 \mid X, o\} \cdot p(X \mid o) \end{aligned} \tag{6.6}$$

where $p(\cdot)$ and $p(\cdot|\cdot)$ denote PDF and conditional PDF, respectively.

It is widely known that $E\{\theta_0 \mid X, o\}$ in (6.6) is [55]

$$E\{\theta_0 \mid X, o\} = \frac{|H^{-1}|^2\sigma^2}{|H^{-1}|^2\sigma^2 + \sigma_D^2}(o - \alpha X) \tag{6.7}$$

and the conditional PDF $p(X \mid o)$ in (6.6) is

$$p(X \mid o) = \frac{p(o \mid X)p(X)}{p(o)}$$

$$
\begin{aligned}
&= \text{const} \cdot p(o \mid X) \\
&= \frac{p(o \mid X)}{\sum_{X' \in \mathcal{X}} p(o \mid X')}
\end{aligned} \tag{6.8}
$$

where

$$
p(o \mid X) = \frac{1}{2\pi(|H^{-1}|^2\sigma^2 + \sigma_D^2)} \exp\left[- \frac{1}{2(|H^{-1}|^2\sigma^2 + \sigma_D^2)} \mid o - \alpha X \mid^2 \right].
$$

After plugging (6.7) and (6.8) into (6.6), we have

$$
E\{\theta_0 \mid o\} = \sum_{X \in \mathcal{X}} \frac{|H^{-1}|^2\sigma^2}{|H^{-1}|^2\sigma^2 + \sigma_D^2}(o - \alpha X) \cdot \frac{p(o \mid X)}{\sum_{X' \in \mathcal{X}} p(o \mid X')}. \tag{6.9}
$$

Second, $E\{\theta_1 \mid o\}$ is expressed as

$$
\begin{aligned}
E\{\theta_1 \mid o\} &= E\{\theta_1 \mid o, \hat{X}\} \\
&= \sum_{X \in \mathcal{X}} (X - \hat{X}) \cdot p(X \mid o) \\
&= \sum_{X \in \mathcal{X}} (X - \hat{X}) \cdot \frac{p(o \mid X)}{\sum_{X' \in \mathcal{X}} p(o \mid X')}.
\end{aligned} \tag{6.10}
$$

Finally, combining (6.9) and (6.10), the MMSE estimator of θ is

$$
\hat{\theta} = \sum_{X \in \mathcal{X}} \left(\frac{|H^{-1}|^2\sigma^2}{|H^{-1}|^2\sigma^2 + \sigma_D^2}(o - \alpha X) + (X - \hat{X}) \right) \cdot \frac{p(o \mid X)}{\sum_{X' \in \mathcal{X}} p(o \mid X')}. \tag{6.11}
$$

For systems in which high computational complexity is not allowed, it is too complicated to use the estimator in (6.11). Thus, we propose the low-complexity version of the MMSE estimator of θ by using the following approximation as

$$
\sum_{X \in \mathcal{X}} X \cdot \frac{p(o \mid X)}{\sum_{X' \in \mathcal{X}} p(o \mid X')} \simeq \hat{X}. \tag{6.12}
$$

By plugging (6.12) into (6.11), the MMSE estimator $\hat{\theta}$ is approximated as

$$\hat{\theta} \simeq \frac{|H^{-1}|^2\sigma^2}{|H^{-1}|^2\sigma^2 + \sigma_D^2}(o - \alpha\hat{X}).$$

In simulations, the above estimator is used for ease of implementation.

6.2.3.3. Selection Criterion of Observations

As we mentioned, based on the estimate of $\theta(k)$, we can select reliable observations which will be used to recover the clipping noise $\mathbf{c}$. Furthermore, we use a selection criterion which selects the observations whose observation noise level is lower than the average noiseless observation power. That is, the following selection criterion is used in the proposed scheme;

$$\mathcal{K} = \{k : |\hat{\theta}(k)|^2 < E\{|C(k)|^2\}\}. \tag{6.13}$$

If the cardinality of $\mathcal{K}$ is M, an $M \times N$ selection matrix $\mathbf{S}$ in (6.4) is constructed by selecting the corresponding M rows from $\mathbf{I}_N$.

6.2.4. Computational Complexity

In terms of computational complexity, the CS reconstruction algorithm part of the proposed scheme is a dominant factor, and each iteration of the OMP algorithm approximately requires the complexity of one N-point FFT because the sensing matrix in (6.4) is an $M \times N$ partial Fourier matrix [52].

For ease of implementation, in the proposed scheme, the number of iterations of the OMP algorithm is a half of the number of average dominant pulses of the clipping noise $\mathbf{c}$ ($0.5 \cdot E\{||\mathbf{c}||_0\}$ for $L = 1$ and $0.5 \cdot E\{N_p\}$

for $L = 4$), based on the discussion in Section 6.2.1. That is, we run the OMP algorithm $0.5N \cdot e^{-\gamma^2}$ times and $0.5N \cdot \sqrt{\frac{\pi}{3}}\gamma e^{-\gamma^2}$ times for $L = 1$ and $L = 4$, respectively. Although this number of iterations seems to be insufficient to recover the whole pulses of the clipping noise, it still shows good performance as shown in Section 6.3. This is because, in practice, the number of dominant pulses in the clipping noise is usually less than the number that we inferred in Section 6.2.1, owing to the fact that an OFDM signal sequence is under the total energy constraint by the Parseval's theorem.

6.3. Simulation Results

In this section, we evaluate the BER performance of the proposed clipping noise cancellation scheme for uncoded OFDM systems. Here, the SNR means the ratio of bit energy to the variance of AWGN. We simulate both the case of clipping at the Nyquist sampling rate ($L = 1$) and the case of clipping and filtering at an oversampling rate ($L = 4$) over an AWGN channel and a Rayleigh fading channel. To confirm the validity of the proposed scheme, we compare the proposed scheme with existing clipping noise cancellation schemes over a Rayleigh fading channel.

6.3.1. AWGN Channel

Fig. 6.2 shows the BER performance of the proposed scheme over an AWGN channel when the clipping at the Nyquist sampling rate and 16-QAM are used. As we mentioned, the proposed scheme can be effectively

adopted for not too small clipping ratio and thus various clipping ratios are used for simulations. Although the proposed scheme shows performance degradation in low SNR region, it clearly shows that the proposed scheme performs well for various clipping ratios in moderate SNR region that we are interested in.

Fig. 6.3 shows the BER performance of the proposed scheme over an AWGN channel when the clipping and filtering at four-times oversampling rate is used. Clipping ratio γ is fixed to $1.5 = 3.52$dB. In this case, the proposed scheme also performs well in moderate SNR region, even though the clipping noise $\mathbf{c}$ is not an exactly sparse signal when oversampling is used. Also, the proposed schemes performs well regardless of the number of subcarriers N.

6.3.2. Rayleigh Fading Channel

In this subsection, we compare the proposed scheme with other clipping noise cancellation schemes over a fading channel. The length of the channel is assumed to be four and the channel taps are assumed to be complex Gaussian distributed with zero-mean and variance 1/4, i.e., frequency-selective fading channel where coefficients of taps are Rayleigh distributed. More precisely, the $N \times 1$ channel impulse response $\mathbf{h}$ is modeled as

$$\mathbf{h} = [h(0), h(1), h(2), h(3), 0, \cdots, 0]^T$$

where $h(0), h(1), h(2), h(3) \sim \mathcal{CN}(0, 1/4)$ and $H(k)$ is the k-th element of $\mathrm{FFT}_N(\mathbf{h})$, a frequency-selective fading channel. We assume the perfect

knowledge of the channel frequency response at the receiver as other works [37], [38].

Figs. 6.4, 6.5, and 6.6 compare the BER performance of the proposed scheme, IEC [37], DAR [38], and TR-CS [28] for two sampling rates and modulations. In Fig. 6.6, only the BER performance of the IEC scheme and the proposed scheme are given because the others do not work when clipping and filtering at an oversampling rate is used. Also, in TR-CS, the OMP algorithm is used for CS reconstruction for a fair comparison. In Fig. 6.5, quadrature phase shift keying (QPSK) and severe clipping ($\gamma = 1.0$) are used in order to show the performance gap clearly. Although the nonzero components of the clipping noise $\mathbf{c}$ becomes too large to keep the sparsity of $\mathbf{c}$, the proposed scheme works well because the dominant pulses of the clipping noise are recovered by CS technique.

Firstly, the tone reservation by CS (TR-CS) scheme in [28] shows poor BER performance due to the weakness of CS reconstruction to the channel noise, although it uses 41 reserved tones out of 128 tones, which seems to be sufficient. Meanwhile, the scheme in [29] uses compressed observations of pilot tones. Thus, from the result, one can expect that the scheme in [29] also shows poor BER performance unless the number of pilot tones is larger than 41, which becomes unpractical. As we discussed, the absence of the selecting process of reliable observations seems to result in poor BER performance of the previous works [28], [29] using CS.

Secondly, the DAR scheme in [38] is the most frequently cited scheme among the clipping noise cancellation schemes outside CS regime. The

DAR scheme shows good BER performance, but it works only for the case when clipping at the Nyquist sampling rate is used. This limitation is a major drawback of the DAR scheme in a practical sense.

Thirdly, the BER performance of the IEC scheme in [37] is also given. The scheme in [37] is based on iterative estimation and cancellation of the clipping noise. In Figs. 6.4, 6.5, and 6.6, the IEC scheme works well for two sampling rates similarly as the proposed scheme. But, in Fig. 6.5, the proposed scheme shows better BER performance than the IEC scheme. In terms of computational complexity, the IEC scheme requires two LN-point FFT / IFFT pairs to recreate the clipping process regardless of the clipping ratio. Thus, the proposed scheme has a computational benefit over the IEC scheme for a large clipping ratio and small N as described in Section 6.2.4.

In Fig. 6.5, the proposed scheme shows the best BER performance compared to the other schemes. Moreover, it is worth noting that the proposed scheme shows better BER performance than the no clipping case. This is because the clipping procedure can reduce the average transmission power compared to no clipping case, and this results in BER performance gain, which is called shaping gain.

Fig. 6.7 compares the BER performance of the proposed scheme and the PR-CS scheme in [51]. In Fig. 6.7, clipping at the Nyquist sampling is used and $\gamma = 1.3$ is used. In PR-CS scheme [51], the number of compressed observations M needs to be optimized. Thus, BER at SNR=35dB is plotted versus the number of compressed observations of PR-CS [51]. Note

that our scheme adaptively sets the number of compressed observations according to (6.13), which is more intelligent than the PR-CS scheme. In PR-CS, the OMP algorithm is used for CS reconstruction for a fair comparison. Clearly, the proposed scheme shows superior BER performance compared to the PR-CS scheme [51].

6.4. Conclusion

In this chapter, a new clipping noise cancellation scheme using CS for OFDM systems is proposed. To reconstruct the clipping noise, the proposed scheme exploits its compressed observations underlying in the data tones less contaminated by channel noise. To do this, an observation noise level in each data tone is estimated by exploiting the statistical model of a clipped signal. The proposed clipping noise cancellation scheme cancels out the clipping noise well over an AWGN channel and a frequency-selective fading channel, which is verified through simulations. Compared with the previously known schemes, the proposed scheme substantially improves the reconstruction performance by adopting the selection of reliable observations.

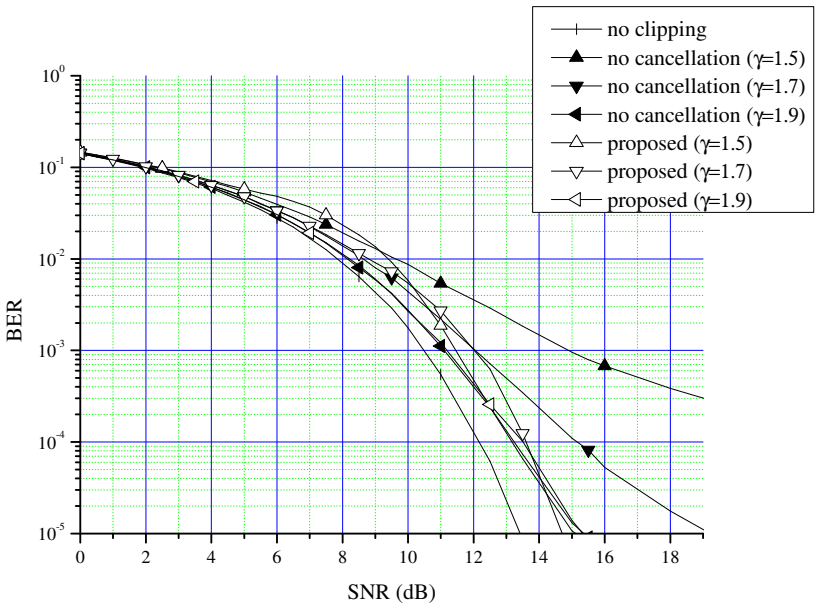

Figure 6.2: BER performance of the proposed scheme for various clipping ratios γ over an AWGN channel when $L = 1$, $N = 128$, and 16-QAM are used.

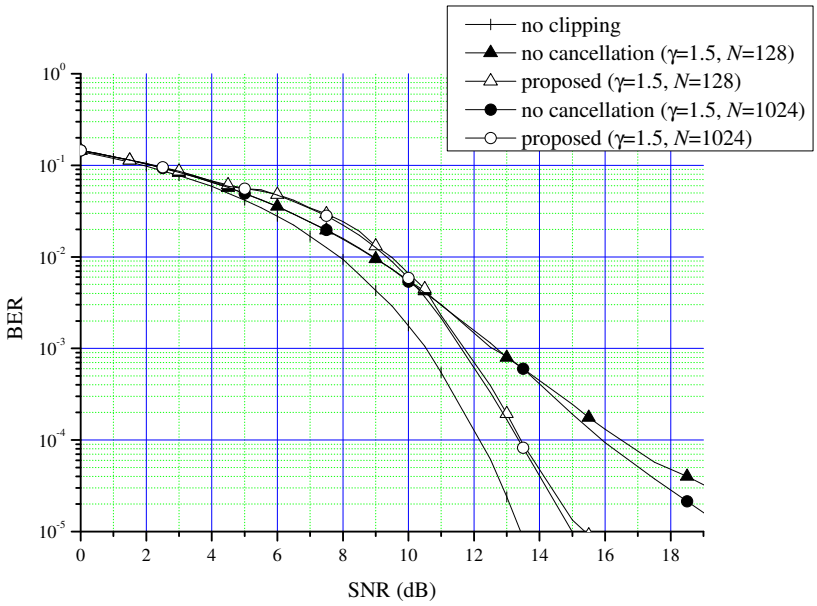

Figure 6.3: BER performance of the proposed scheme for various N over an AWGN channel when $L = 4$ and 16-QAM are used.

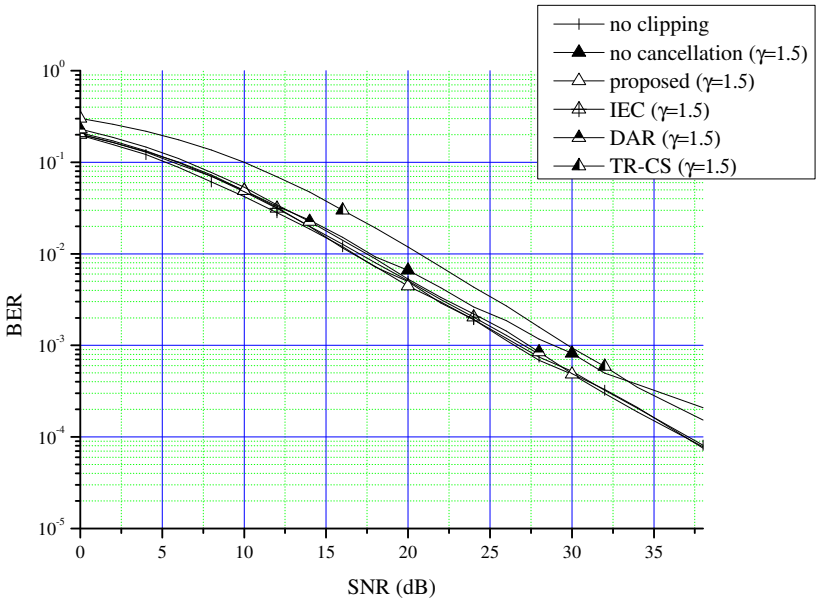

Figure 6.4: BER comparison of the proposed scheme and the existing clipping noise cancellation schemes (IEC [37], DAR [38], and TR-CS [28]) over a frequency-selective fading channel when $L = 1$, $N = 128$, and 16-QAM are used.

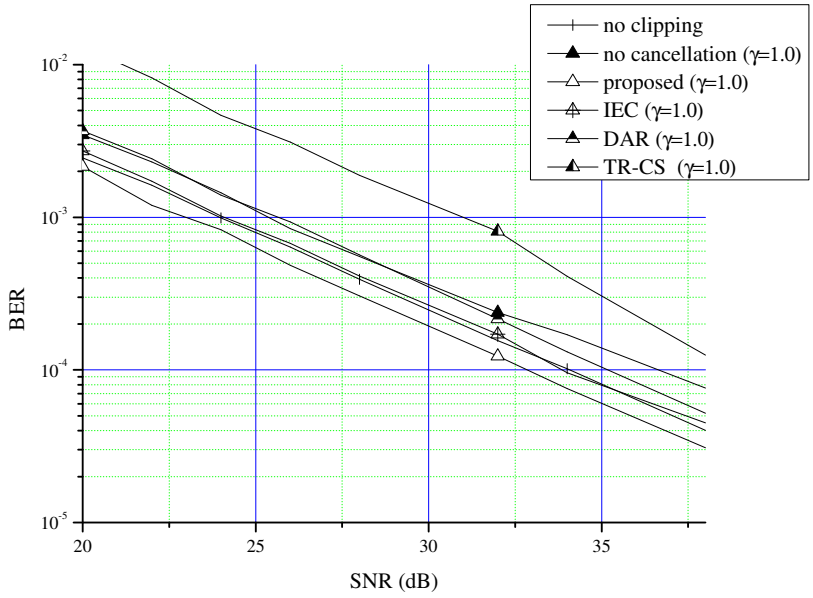

Figure 6.5: BER comparison of the proposed scheme and the existing clipping noise cancellation schemes (IEC [37], DAR [38], and TR-CS [28]) over a frequency-selective fading channel when $L = 1$, $N = 128$, and QPSK are used.

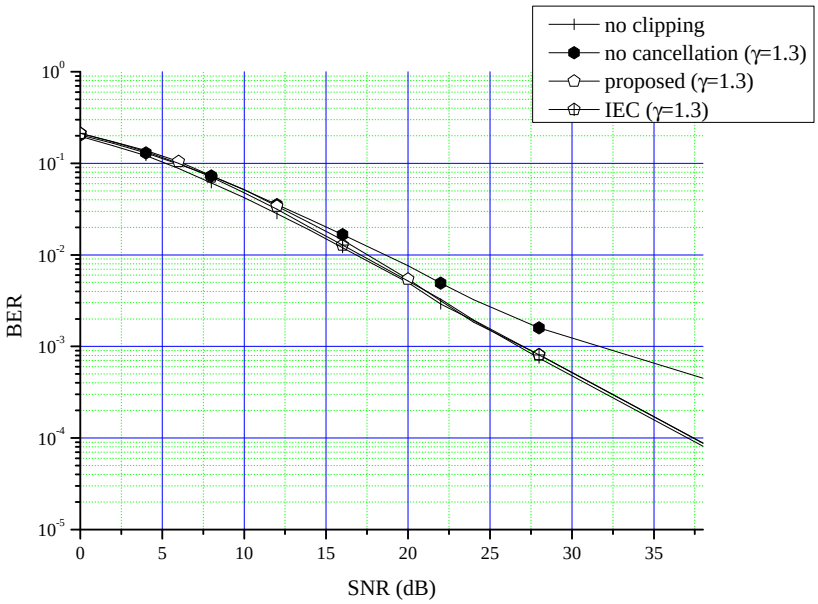

Figure 6.6: BER comparison of the proposed scheme and the IEC scheme [37] over a frequency-selective fading channel when $L = 4$, $N = 128$, and 16-QAM are used.

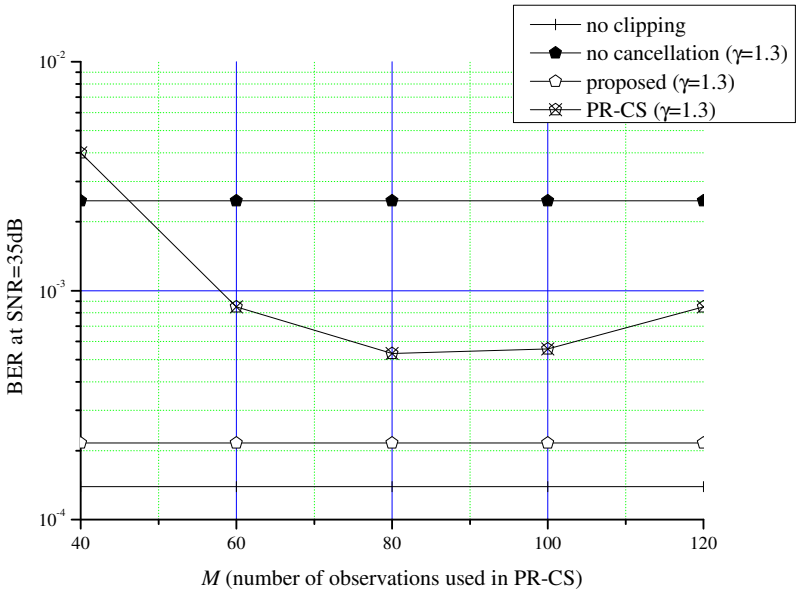

Figure 6.7: BER comparison of the proposed scheme and the PR-CS scheme [51] over a frequency-selective fading channel when $L = 1$, $N = 128$, and 16-QAM are used.

Chapter 7. Conclusions

In this dissertation, we reviewed OFDM system and their PAPR characteristics. To solve PAPR problem of OFDM system, several PAPR reduction schemes have been proposed. These PAPR reduction schemes such as coding, clipping and filtering, SLM, PTS, and TR are introduced and have their own characteristics and trade-off.

In Chapter 4, the new low-complexity SLM scheme exploiting the signals at an intermediate stage of IFFT is proposed, which shows almost the same PAPR reduction performance as the conventional SLM scheme when $i = 2$. Instead of performing U IFFTs as in the conventional SLM scheme, the proposed scheme operates one IFFT up to $(n - i)$ stages, which is common to generation of all alternative OFDM signal sequences. Then, the connections in each subblock at the stage $(n - i)$ of IFFT is cyclically shifted by the predetermined shift value in the proposed SLM scheme. Since the cyclic shifts at an intermediate stage of IFFT can be viewed as multiplying an equivalent phase rotation vector consisting of complex numbers with a unit magnitude to the input symbol sequence, there is no BER degradation compared to the conventional SLM scheme. Therefore, the proposed SLM scheme can be a good choice among many PAPR reduction schemes if the most important criterion of the PAPR reduction to consider is BER performance.

In Chapter 5, we propose the ES method for various SLM schemes. When various SLM schemes generate alternative OFDM signal sequences, the proposed ES method selects the transmitted OFDM signal sequence efficiently. Aided by the ES method, the alternative OFDM signal components are sequentially generated and the generation procedure can be interrupted according to the component power value. As a result, the average computational complexity of the SLM schemes is substantially reduced. It is meaningful to mention that the application of the proposed ES method does not degrade the PAPR reduction performance of the used SLM scheme.

We described how to apply the ES method to the conventional SLM scheme and analyzed its computational complexity. Furthermore, we briefly described the application of the proposed ES method to the three low-complexity SLM schemes and simulation results confirmed the computational benefit of the ES method. We anticipate that the proposed ES method can be effectively applied to many other SLM schemes.

In Chapter 6, the new clipping noise cancellation scheme using CS for OFDM systems is proposed. To reconstruct the clipping noise, the proposed scheme exploits its compressed observations underlying in the data tones less contaminated by channel noise. To do this, an observation noise level in each data tone is estimated by exploiting the statistical model of a clipped signal. The proposed clipping noise cancellation scheme cancels out the clipping noise well over an AWGN channel and a frequency-selective fading channel, which is verified through simulations. Compared

with the previous schemes, the proposed scheme substantially improves the reconstruction performance by adopting the selection of reliable observations.

Bibliography

[1] R. W. Chang and R. A. Gibby, "A theoretical study of performance of an orthogonal multiplexing data transmission scheme," *IEEE Trans. Commun.*, vol. 16, no. 4, pp. 529–540, Aug. 1968.

[2] S. B. Weinstein and P. M. Erbert, "Data transmission by frequency-division multiplexing using the discrete Fourier transform," *IEEE Trans. Commun.*, vol. 19, no. 4, pp. 628–634, Oct. 1971.

[3] A. Peled and A.Ruiz, "Frequency domain data transmission using reduced computational complexity algorithms," in *Proc. IEEE ICASSP,* Denver CO, Apr. 1980, pp. 964–967.

[4] R. van Nee and R. Prasad, *OFDM for Wireless Multimedia Communications.* Boston, MA: Arthech House, 2000.

[5] D.-W. Lim, S.-J. Heo, and J.-S. No, "An overview of peak-to-average power ratio reduction schemes for OFDM signals," *J. Commun. Netw.,* vol. 11, no. 3, pp. 229–239, Jun. 2009.

[6] Y. Louet and J. Palicot, "A classification of methods for efficient power amplification of signals," *Ann. Telecommun.*, vol. 63, no 7–8, pp. 351–368, Aug. 2008.

[7] R. O'neal and L. N. Lopes, "Envelope variation and spectral splatter in clipped multicarrier signals," in *Proc. IEEE PIMRC*, Toronto, Canada, Sep. 1995, pp. 71–75.

[8] X. Li and L. Cimini, "Effects of clipping and filtering on the performance of OFDM," *IEEE Commun. Lett.,* vol. 2, no. 5, pp. 131–133, May 1998.

[9] D. Guel and J. Palicot, "Analysis and comparison of clipping techniques for OFDM peak-to-average power ratio reduction," in *Proc. Int. Conf. on DSP*, Santorini, Greece, Jul. 2009, pp. 1–6.

[10] J. A. Davis and J. Jedwab, "Peak-to-mean power control in OFDM, Golay complementary sequences, and Reed.Muller codes," *IEEE Trans. Inf. Theory,* vol. 45, no. 7, pp. 2397–2417, Nov. 1999.

[11] Y.-C. Tsai, S.-K. Deng, K.-C. Chen, and M.-C. Lin, "Turbo coded OFDM for reducing PAPR and error rates," *IEEE Trans. Wireless Commun.*, vol. 7, no. 1, pp. 84–89, Jan. 2008.

[12] O. Daoud and O. Alani, "Reducing the PAPR by utilisation of the LDPC code," *IET Commun.*, vol. 3, no. 4, pp. 520–529, Apr. 2009.

[13] B. S. Krongold and D. L. Jones, "PAR reduction in OFDM via active constellation extension," *IEEE Trans. Broadcast.*, vol. 49, no. 3, pp. 258–268, Sep. 2002.

[14] J. Tellado, "Peak to average power reduction for multicarrier modulation," Stanford University, Stanford, CA, 2000, Ph.D. dissertation.

[15] D. Guel, J. Palicot, and Y. Louet, "Tone reservation technique based on geometric method for orthogonal frequency division multiplexing peak-to-average power ratio reduction," *IET Commun.*, vol. 4, no. 17, pp. 2065–2073, Nov. 2010.

[16] S. H. Müller, R. W. Bäuml, R. F. H. Fischer, and J. B. Huber, "OFDM with reduced peak-to-average power ratio by multiple signal representation," *Ann. Telecommun.*, vol. 52, no. 1–2, pp. 58–67, Feb. 1997.

[17] A. Mobasher and A.K. Khandani, "Integer-based constellation-shaping method for PAPR reduction in OFDM systems," *IEEE Trans. Commun.*, vol. 54, no. 1, pp. 119–127, Jan. 2006.

[18] R. W. Bäuml, R. F. H. Fischer, and J. B. Huber, "Reducing the peak-to-average power ratio of multicarrier modulation by selected mapping," *Electron. Lett.*, vol. 32, no. 22, pp. 2056–2057, Oct. 1996.

[19] S. Y. L. Goff, S. S. Al-Samahi, B. K. Khoo, C. C. Tsimenidis, and B. S. Sharif, "Selected mapping without side information for PAPR reduction in OFDM," *IEEE Trans. Wireless Commun.*, vol. 8, no. 7, pp. 3320–3325, Jul. 2009.

[20] S.-J. Heo, H.-S. Noh, J.-S. No, and D.-J. Shin, "Modified SLM scheme with low complexity for PAPR reduction of OFDM systems," *IEEE Trans. Broadcast.*, vol. 53, no. 4, pp. 804–808, Dec. 2007.

[21] H.-B. Jeon, K.-H. Kim, J.-S. No, and D.-J. Shin, "Bit-based SLM schemes for PAPR reduction in QAM modulated OFDM signals," *IEEE Trans. Broadcast.*, vol. 55, no. 3, pp. 679–685, Sep. 2009.

[22] C.-L. Wang and S.-J. Ku, "Novel conversion matrices for simplifying the IFFT computation of an SLM-based PAPR reduction scheme for OFDM systems," *IEEE Trans. Commun.*, vol. 57, no. 7, pp. 1903–1907, Jul. 2009.

[23] Z. Du, N. C. Beaulieu, and J. Zhu, "Selected time-domain filtering for reduced-complexity PAPR reduction in OFDM," *IEEE Trans. Veh. Technol.*, vol. 60, no. 3, pp. 1170–1176, Mar. 2009.

[24] H.-B. Jeon, J.-S. No, and D.-J. Shin, "A low-complexity SLM scheme using additive mapping sequences for PAPR reduction of OFDM signals," *IEEE Trans. Broadcast.*, vol. 57, no. 4, pp. 866–875, Dec. 2011.

[25] D.-W. Lim, J.-S. No, C.-W. Lim, and H. Chung, "A new SLM OFDM scheme with low complexity for PAPR reduction," *IEEE Signal Process. Lett.*, vol. 12, no. 2, pp. 93–96, Feb. 2005.

[26] A. Ghassemi and T. A. Gulliver, "Partial selective mapping OFDM with low complexity IFFTs," *IEEE Comm. Lett.*, vol. 12, no. 1, pp. 4–6, Jan. 2008.

[27] R. J. Baxely and G. T. Zhou, "MAP metric for blind phase sequence detection in selected mapping," *IEEE Trans. Broadcast.*, vol. 51, no. 4, pp. 565–570, Dec. 2005.

[28] E. B. Al-Safadi and T. Y. Al-Naffouri, "Peak reduction and clipping mitigation in OFDM by augmented compressive sensing," *IEEE Trans. Signal Process.,* vol. 60, no. 7, pp. 3834–3839, Jul. 2012.

[29] M. Mohammadnia-Avval, A. Ghassemi, and L. Lampe, "Compressive sensing recovery of nonlinearity distorted OFDM signals," in *Proc. IEEE Int. Conf. Commun.*, Kyoto, Japan, Jun. 2011, pp. 1–5.

[30] R. van Nee and A. de Wild, "Reducing the peak-to-average power ratio of OFDM," in *Proc. VTC*, Ottawa, Canada, May 1998, pp. 2072–2076.

[31] H. Ochiai and H. Imai, "On the distribution of the peak-to-average power ratio in OFDM signals," *IEEE Trans. Commun.*, vol. 49, no. 2, pp. 282–289, Feb. 2001.

[32] M. Sharif, M. G.-Alkansari, and B. H. Khalaj, "On the peak-to-average power of OFDM signals based on oversampling," *IEEE Trans. Commun.*, vol. 51, no. 1, pp. 72–78, Jan. 2003.

[33] H. Ochiai and H. Imai, "Performance of the deliberate clipping with adaptive symbol selection for strictly band-limited OFDM systems," *IEEE J. Sel. Areas Commun.*, vol. 18, no. 11, pp. 2270–2277, Nov. 2000.

[34] P. Banelli and S. Cacopardi, "Theoretical analysis and performance of OFDM signals in nonlinear AWGN channels," *IEEE Trans. Commn.,* vol. 48, no. 3, pp. 430–441, Mar. 2000.

[35] H. Ochiai and H. Imai, "Performance analysis of deliberately clipped OFDM signals," *IEEE Trans. Commun.*, vol. 50, no. 1, pp. 89–101, Jan. 2002.

[36] E. Costa, M. Midrio, and S. Pupolin, "Impact of amplifier nonlinearities on OFDM transmission system performance," *IEEE Commun. Lett.*, vol. 3, no. 2, pp. 37–39, Feb. 1999.

[37] H. Chen and A. Haimovich, "Iterative estimation and cancellation of clipping noise for OFDM signals," *IEEE Commun. Lett.*, vol. 7, no. 7, pp. 305–307, Jul. 2003.

[38] D. Kim and G. L. Stuber, "Clipping noise mitigation for OFDM by decision-aided reconstruction," *IEEE Commun. Lett.*, vol. 3, no. 1, pp. 4–6, Jan. 1999.

[39] D.-W. Lim, S.-J. Heo, J.-S. No, and H. Chung, "On the phase sequences of SLM OFDM system for PAPR reduction," in *Proc. ISITA 2004*, Parma, Italy, Oct. 2004, pp. 230–235.

[40] S.-J. Heo, H.-S. Joo, J.-S. No, D.-W. Lim, and D.-J. Shin, "Analysis of PAPR reduction performance of SLM schemes with correlated phase vectors," in *Proc. IEEE ISIT*, Seoul, Korea, Jun. 2009, pp. 1540–1543.

[41] A. V. Oppenheim, R. W. Schafer, and J. R. Buck, *Discrete-Time Signal Processing*. Upper Saddle River, NJ: Prentice-Hall, 1998.

[42] H. Saeedi, M. Sharif, and F. Marvasti, "Clipping noise cancellation in OFDM systems using oversampled signal reconstruction," *IEEE Commun. Lett.*, vol. 6, no. 2, pp. 73–75, Feb. 2002.

[43] R. AliHemmati and P. Azmi, "Iterative reconstruction-based method for clipping noise suppression in OFDM systems," *IEE Proc. Commun.*, vol. 152, no. 4, pp. 452–456, Aug. 2005.

[44] U.-K. Kwon, D. Kim, and G.-H. Im, "Amplitude clipping and iterative reconstruction of MIMO-OFDM signals with optimum equalization," *IEEE Trans. Wireless Commun.,* vol. 8, no. 1, pp. 268–277, Jan. 2009.

[45] Y. Chen, J. Zhang, and A. D. S. Jayalath, "Estimation and compensation of clipping noise in OFDMA systems," *IEEE Trans. Wireless Commun.,* vol. 9, no. 2, pp. 523–527, Feb. 2010.

[46] D. L. Donoho, "Compressed sensing," *IEEE Trans. Inf. Theory*, vol. 52, no. 4, pp. 1289–1306, Apr. 2006.

[47] E. Candes, J. Romberg, and T. Tao, "Stable signal recovery from incomplete and inaccurate measurements," *Comm. Pure Appl. Math.*, vol. 59, no. 8, pp. 1207–1223, Aug. 2006.

[48] E. Candes and T. Tao, "Near-optimal signal recovery from random projections: universal encoding strategies?," *IEEE Trans. Inf. Theory*, vol. 52, no. 12, pp. 5406–5425, Dec. 2006.

[49] S. J. Wright, R. D. Nowak, and M. A. T. Figueiredo, "Sparse reconstruction by separable approximation," *IEEE Trans. Signal Process.*, vol. 57, no. 7, pp. 2479–2493, Jul. 2009.

[50] E. B. Al-Safadi and T. Y. Al-Naffouri, "On reducing the complexity of tone reservation based PAPR reduction schemes by compressive sensing," in *Proc. IEEE Globecom 2009*, Honolulu HI, Nov. 2009, pp. 1–6.

[51] E. B. Al-Safadi and T. Y. Al-Naffouri, "Pilotless recovery of nonlinearly distorted OFDM signals by compressive sensing over reliable data carriers," in *Proc. IEEE Int. Workshop on SPAWC*, Cesme, Turkey, Jun. 2012, pp. 580–584.

[52] J. A. Tropp and A. C. Gilbert, "Signal recovery from random measurements via orthogonal matching pursuit," *IEEE Trans. Inf. Theory*, vol. 53, no. 12, pp. 4655–4666, Dec. 2007.

[53] L. Wang and C. Tellambura, "Analysis of clipping noise and tone-reservation algorithms for peak reduction in OFDM systems," *IEEE Trans. Veh. Technol.*, vol. 57, no. 3, pp. 1675–1694, May 2008.

[54] T. Tony Cai and Lie Wang, "Orthogonal matching pursuit for sparse signal recovery with noise," *IEEE Trans. Inf. Theory*, vol. 57, no. 7, pp. 4680–4688, Jul. 2011.

[55] S. M. Kay, *Fundamentals of Statistical Signal Processing: Estimation Theory*. Upper Saddle River, NJ: Prentice-Hall, 1993.

초 록

본 논문은 직교주파수분할다중화 (OFDM) 시스템의 최대전력대평균전력비 (PAPR) 를 감소시키는 저복잡도 선택사상기법 (SLM) 및 이러한 SLM 기법들에서 효율적으로 전송 OFDM 신호 수열을 선택하는 방법, 그리고 클리핑 (clipping) 기법 사용시 수신단에서 클리핑으로 인한 왜곡을 제거하는 새로운 기법들을 차례로 제안한다. 먼저 서두에서는 OFDM 시스템의 기본원리와 성능 및 구현방법 등을 살펴본다. OFDM 신호는 일반적으로 높은 PAPR을 갖는데 이는 OFDM 시스템의 큰 단점으로 꼽힌다. 따라서, PAPR을 감소시키는 기법에 관한 연구가 지금까지 활발히 진행되어 왔으며 대표적인 방법으로는 클리핑 기법, SLM, 부분전송수열 (PTS), 톤 예약 기법 (TR), 톤 삽입 기법 (TI) 등이 있다.

첫 번째로 본 논문에서는, 적은 복잡도를 가지는 새로운 SLM 기법을 제안한다. 이 기법은 역퓨리에 변환 (IFFT) 구조의 중간 단계의 각 부분 구조 사이의 신호들을 순환 이동 시킴으로써, 후보 OFDM 신호 수열들을 발생시킨다. 기존의 SLM 기법과 비교하였을때에, 제안하는 SLM 기법은 비슷한 PAPR 감소 성능을 갖으면서도, 낮은 계산 복잡도를 요구한다. 제안하는 기법의 성능은 모의 실험을 통하여 검증되었으며, 자세한 설계 인자들에 대해서는 수학적으로 분석하였다.

두 번째로 본 논문에서는, 여러 SLM 기법에서 후보 OFDM 신호 수열들중에 전송 OFDM 신호 수열을 선택 하는데에 있어, 이를 효율적이게 수행하는 방법을 제안하였다. 제안하는 효율적인 선택 방법은 OFDM 시스템에서 쓰이는 IFFT 구조를 활용하여, 후보 OFDM 신호 수열들 생성중 이 신호들의 크기를 관찰하여 생성 과정을 필요에 따라 중단시킨다.

그 결과로, 이 효율적인 선택 방법은 여러 SLM 기법들의 계산 복잡도를 상당히 감소 시킬 수 있다. 또한 PAPR 감소 성능의 열화가 없어 더욱 의미가 있다.

세 번째로 본 논문에서는, OFDM 시스템에서 송신단에서 PAPR 감소를 위하여 클리핑이 이루어졌을 경우, 수신단에서 압축센싱 (CS) 기법을 활용하여 클리핑 잡음을 제거하는 기법을 제안한다. 제안하는 기법은 기존의 기법들과 다르게, 파일럿 톤들이나 예약된 톤들을 필요로 하지 않는다. 대신, 데이터 톤들에 존재하는 클리핑 잡음의 측정 값들을 활용하게 된다. 또한 이러한 측정 값들을 활용함에 있어, 복원 과정에 대한 채널 잡음의 악영향을 최소화 시키기 위하여 신뢰도가 높은 측정 값들만을 선택적으로 취하게 된다. 모의 실험 결과는 제안하는 기법이 기존의 클리핑 잡음 제거 기법들에 비하여 우수한 성능을 보여준다.

주요어: 클리핑, 압축센싱, 직교주파수분할다중화, 최대전력대평균전력비, 선택사상기법.

학번: 2010-30210